AD-A148 742 STABILITY OF LOW EMBANKMENTS ON SOFT CLAY PART 2 STUDIES OF VANE AND PENE..(U) CAMBRIDGE UNIV (ENGLAND) DEPT OF ENGINEERING M S ALMEIDA ET AL. NOV 84 1/1

UNCLASSIFIED DAJA37-82-C-0177 F/G 8/13 NL

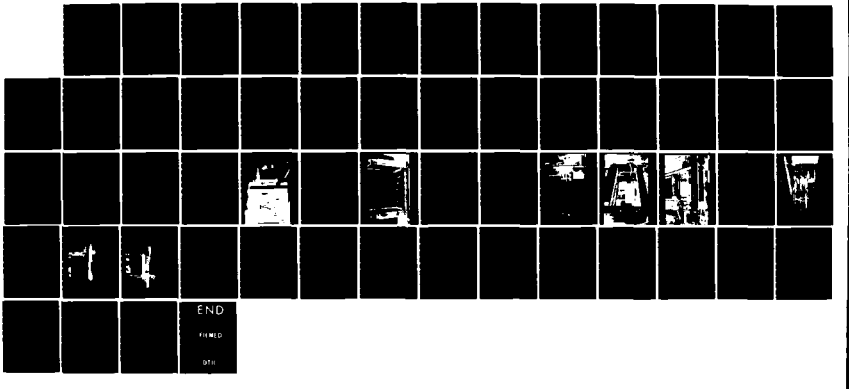

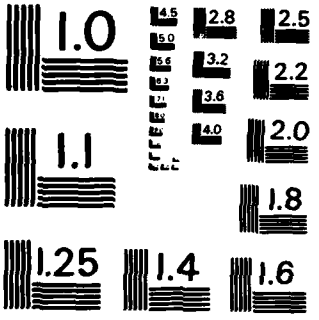

STABILITY OF EMBANKMENTS ON SOFT CLAY

Final Technical Report

Part 2 of 3: Studies of vane and penetrometer tests during centrifuge flight

by

M S S Almeida and R H G Parry

November 1984

United States Army

EUROPEAN RESEARCH OFFICE OF THE U S ARMY

London, England

CONTRACT NUMBER DAJ A37-82-C-0177

Cambridge University Engineering Department

SECURITY CLASSIFICATION OF THIS PAGE (When Data Entered)

REPORT DOCUMENTATION PAGE		READ INSTRUCTIONS BEFORE COMPLETING FORM
1. REPORT NUMBER	2. GOVT ACCESSION NO. AD-A145 742	3. RECIPIENT'S CATALOG NUMBER
4. TITLE (and Subtitle) Stability of low embankments on soft clay; Part 2 of 3: Studies of Vane and Penetrometer tests during Centrifuge Flight		5. TYPE OF REPORT & PERIOD COVERED Final Technical Report 6. PERFORMING ORG. REPORT NUMBER
7. AUTHOR(s) M S S Almeida and R H G Parry		8. CONTRACT OR GRANT NUMBER(s) DAJA37-82-C-0177
9. PERFORMING ORGANIZATION NAME AND ADDRESS Cambridge University Engineering Department Trumpington Street, Cambridge, UK CB2 1PZ		10. PROGRAM ELEMENT, PROJECT, TASK AREA & WORK UNIT NUMBERS 61102A-IT161102-BH57-01
11. CONTROLLING OFFICE NAME AND ADDRESS USARDSG-UK Box 65, FPO New York, NY 09510		12. REPORT DATE October 1983 13. NUMBER OF PAGES 56
14. MONITORING AGENCY NAME & ADDRESS(if different from Controlling Office)		15. SECURITY CLASS. (of this report) Unclassified 15a. DECLASSIFICATION/DOWNGRADING SCHEDULE

16. DISTRIBUTION STATEMENT (of this Report)

Approved for public release; distribution unlimited

17. DISTRIBUTION STATEMENT (of the abstract entered in Block 20, if different from Report)

18. SUPPLEMENTARY NOTES

19. KEY WORDS (Continue on reverse side if necessary and identify by block number)

centrifuge, clay, coefficient of consolidation, dissipation, overconsolidation ratio, piezocone, pore pressure, shaft friction, testing rates, undrained shear strength

20. ABSTRACT (Continue on reverse side if necessary and identify by block number)

Correct assessment of soil parameters in centrifuge tests requires these to be measured during flight, and small vane and penetrometer devices have been developed for this purpose. The vane is fixed in position, but the penetrometer can traverse the length of the model, allowing tests to be made a different locations. A programme of tests has been conducted in the centrifuge at 100 g investigating the use of these test methods in consolidated beds of clay. Rate effects are studied for both types of tests and correlations made between cone

DD FORM 1 JAN 73 1473 EDITION OF 1 NOV 65 IS OBSOLETE

resistance and undrained shear strength measured by the vane. A number of penetration tests were also performed to show the progressive increase in strength of a clay bed under staged embankment construction.

Contents

1. Introduction

A series of tests investigating the performance of embankments on soft clay is being performed on the Cambridge centrifuge. An essential feature of this work is the correct determination of the undrained shear strength of the soft clay. This report is concerned with use of vane and penetrometer tests to determine this strength during flight.

If correct strengths of clay beds used for centrifuge tests are to be obtained it is necessary to measure these during centrifuge flight, as pointed out by Davies and Parry (1982). This point is illustrated in fig. 1.1 where vane strengths in a kaolin clay bed during flight and after stopping the centrifuge are shown.

As the position of the vane apparatus in the centrifuge package is fixed, only one determination of the clay strength profile can be carried out in the course of a test. Therefore a penetrometer apparatus has been developed for the determination of the clay resistance at different locations during the centrifuge test. This equipment makes it possible to measure not only the resistance of the virgin foundation but also the corresponding gain of resistance during progress of an embankment construction in stages.

Improved versions of miniature vane and penetrometer probes have been devised to be used during centrifuge tests. A detailed study with these tests in the laboratory in a natural gravity field was the subject of a previous report (Almeida and Parry, 1983).

The apparatus used at Cambridge for centrifugal modelling of embankments on soft clay, together with the vane apparatus Mark II and the new penetrometer apparatus are described in section 2. In section 3 vane and penetrometer tests performed during centrifuge flight are discussed and the results correlated. The influences of both rate of rotation and rate of penetration are illustrated. Penetrometer tests performed during stage construction of the embankment and the resulting gain of strength under the embankment are presented in section 4.

2. Apparatus and experimental procedure

The package used at present in Cambridge for centrifugal modelling of embankments on clay foundation is shown in fig. 2.1 mounted to the centrifuge arm during flight. The package, fig. 2.2 and fig. 2.3, consists of: (a) a rectangular strong box in which a clay cake 0.675 m long by 0.2 m wide and 0.16 m deep is contained; (b) a hopper designed to place a sand embankment in flight in one or more lifts to model stage construction of the embankment; (c) vane apparatus Mark II for the determination of the clay strength in flight at the completion of the consolidation run; (d) a penetrometer which can transverse the length of the strong box.

Strong box and hopper were designed by Horner (1982) and the vane apparatus Mark I was designed by Davies (1981). The upgraded version of the vane Mark II as well as the penetrometer apparatus were developed by Almeida. Preparation of the clay samples as well as the above apparatus are described in the following sections.

2.1 Consolidometer and strong box

The apparatus for the preparation of clay samples for centrifuge tests has been described in detail by Davies (1981) and Horner (1982), and the main features only will be outlined here. The apparatus consists of consolidometer, liner and strong box.

The consolidometer, fig. 2.4, can be dismantled, and side and bottom plates assembled around the liner, which allows the clay cake to be transferred from the consolidometer to the strong box without disturbance. Internal dimensions of the liner are 675 mm long, by 200 mm wide, by 847 mm deep. Clay is introduced as a slurry through the top of the consolidometer, the piston is placed on top of the slurry, and pressure applied by a hydraulic jack connected to a nitrogen gas bottle. Holes in the piston allows drainage towards the top. Downward drainage is permitted through drainage sinks at the bottom of the liner.

After consolidation in the laboratory the clay sample and liner are transferred to the strong box for testing. Internal dimensions of the

strong box are the same as the external dimensions of the liner. Liner and strong box without perspex window are shown in fig. 2.5. A hole drilled inside the liner at the height corresponding to the top of the clay and connected to a pipe running at one side of the liner allows drainage towards the top during testing. Both top and bottom drainage systems of the liner are connected to an external reservoir which controls the water level of the clay sample during testing.

2.2 Preparation of the clay samples

Clay cakes prepared for the present programme consisted of a layered foundation of Gault clay overlying kaolin clay. Gault clay is used on the top of kaolin to produce a stiffer crust. The procedure of preparation of the clay cakes, (Davies, 1981), is described below. The stress history of clay cake SI3 is shown in fig. 2.6.

Kaolin slurry at a nominal water content of 120% is put in the rectangular consolidometer and levelled off at the required height. Gault clay slurry at a nominal water content of 90% is carefully placed on the top of the kaolin slurry. The two clays are consolidated together in stages up to 54 kPa, which takes about ten days.

After consolidation is completed under the final pressure, PDCR81 Druck pore pressure tranducers are inserted through the back of the clay model. Before the removal of pressure from the consolidometer, water which has drained to the top of the consolidometer is removed and the bottom reservoir is disconnected to minimize the amount of water available to be drawn into the clay by the suction created when the sample is unloaded. The pressure is then released and the back plate is carefully removed from the consolidometer in order to produce negligible disturbance to the clay sample. Pore pressure transducers are inserted into holes augered into the clay and then backfilled with thick slurry, a technique commonly used at Cambridge, as described in detail by Davies (1981). Following this the back plate is liberally regreased and the consolidometer reassembled. The transducer leads are taken out of the consolidometer through a groove cut in the piston. The pressure is then reapplied for a further few days.

In order to produce a stiff crust the clay is subsequently subjected to a partial consolidation in the laboratory. A vertical pressure of 150 kPa with drainage permitted only at the top is applied for about two hours. Measurements of pore pressures inside the clay cake allow the σ'_v profile to be determined, as shown in fig. 2.6a. When kaolin alone was used in the early models prepared by Davies (1981), he noticed that following unloading the clay did not retain a high undrained strength at the surface. This was attributed to the inability of the highly permeable kaolin to sustain high suctions. Since Gault clay has smaller voids than kaolin, it can sustain high suctions, consequently retaining higher undrained strengths. The thickness of the clay cake at the end of the consolidation in the laboratory press is about 160 mm, of which the top 40 mm is Gault clay and the bottom 120 mm is kaolin.

Following the consolidation in the laboratory press the clay cake is unloaded and transferred to the strong box. A 9 mm layer of 30/52 Leighton Buzzard sand is placed on the top of the clay sample. The strong box is then mounted onto the centrifuge where it is subjected to an acceleration of 100 g. The purpose of the sand layer is to provide some pressure at the top of the clay sample, so avoiding full swelling to zero pressure under 100 g. This pressure is 8 kPa at 100 g acceleration (see fig. 2.6a). The presence of this surcharge also makes analyses using Cam-clay models easier to perform, since numerical methods using these models do not handle zero effective stresses.

Pore pressure transducers embedded in the clay allow consolidation progress to be monitored. Equilibrium is achieved after about 9 hours of continuous centrifuge run. Values of σ'_v at equilibrium are shown in fig. 2.6a. The resulting overconsolidation ratio varies from 18 at the surface to 1 at a depth of 90 mm, as shown in fig. 2.6b. At prototype scale it consists of a 16 m soft clay foundation, of which the top 9 m layer is overconsolidated and the bottom 7 m layer is normally consolidated.

The relevant clay models tested are listed in table 2.1. Stress histories of models MA3, MA4, MA5 and MA6 are similar to model SI3 presented in fig. 2.6. After the consolidation run in the centrifuge the clay models were subjected to vane tests, penetrometer tests or both (see

table 2.1), to assess the clay strength induced by the stress history. Penetrometer tests were also performed during embankment construction in clay models MA3 and MA6.

2.3 Vane apparatus

The vane apparatus Mark II used here is an improved version of the Mark I apparatus described by Davies(1981) and Davies and Parry(1982).

The apparatus, fig. 2.7, consists of the main frame with triangular spacing plates at both ends and a moving platform in between the spacing plates. A 15 volt DC motor connected to a gearing system drives the moving platform and hence the vane at a constant rate of 0.25 mm/s into the clay. The moving platform is triangular in plan and moves vertically guided by three vertical rods. A DC potentiometer displacement transducer fixed to the top of the frame monitors the vertical movement of the platform, and thus the penetration of the vane. Because of the settlement occurring during in flight consolidation, an additional displacement transducer for settlement is necessary, so that the vane can be inserted to the required depth below the ground surface. A 6 volt DC reversible motor connected to the vane shaft through a bearing rotates the vane at 72^{o}/min. The vane apparatus is seen in fig. 2.8 bolted to the hopper.

The improvements over the Mark I device developed by Davies (1981), as described in detail by Almeida and Parry (1983) are (fig.2.7 and fig.2.8): (a) blades of smaller heights(18 mm dia by 14 mm high) which make possible a better definition of the strength profile by providing more data points; (b) direct measurement of the rate of rotation using a rotary potentiometer and nylon gears connected to the potentiometer and vane shaft; (c) separation of the torques mobilized by blades and shaft using a slip coupling.

The vane shaft is hollow at its top and over a length of 10 mm near the top a thinner wall was machined and four strain gauges bonded to measure torque. Before testing the shaft is lubricated with silicone grease.

2.4 Penetrometer apparatus

A new penetrometer apparatus capable of moving to different positions in plan across the strong box has been developed. The penetrometer test was chosen for the new movable apparatus because it can be carried out more quickly than vane tests and produces a full profile of the soil resistance. Moreover the use of a penetrometer probe as opposed to a vane probe simplifies the design of the apparatus, since the rotation of the vane requires the incorporation of an additional drive mechanism. A disadvantage of the penetrometer test is the need for calibration against vane tests to provide information about the soil strength. However calibration tests can be performed both in laboratory and in the centrifuge and this point is discussed later.

The penetrometer apparatus was positioned between hopper and strong box, as shown in fig. 2.2 The three basic components of the cone penetrometer apparatus, fig. 2.9 and fig. 2.10, are: (a) the horizontal drive system to move the penetrometer carriage across the box; (b) a curved track supporting the carriage; (c) the carriage supporting the cone penetrometer, which is driven in the radial direction of the gravity field by a motor mounted on the carriage. The horizontal drive system, fig.2.11, consists of a motor driving, through a set of pulleys and chains, two lead screws connected to the carriage.

The curved track was incorporated so that the axis of the penetrometer coincided with the direction of the radial gravity field. This design means that penetrometer and load cells are subjected to smaller bending stresses and minimize the power needed to drive the carriage. The lead screws used to move the carriage across the box are simply supported by rotating bearings in one of the track ends and are allowed to float up and down in a groove inside the track, fig. 2.12, as the carriage moves. Nylon brushes bolted to the curved track prevent sand falling from the hopper onto the track interfering with the movement of the carriage.

The motor driving the carriage is a Parvalux 210 volt DC shunt wound motor positioned at the back of the penetrometer apparatus. The motor is operated from the control room by a control box with variable speed

range and a capability of reversing the motor.

It is possible to monitor the position of the carriage on the track by an optical system consisting of a slotted disc attached to one of the lead screws which passes through an optical switch, as shown in fig. 2.11.

The pulses generated by the slotted disc moving through the optical switch are converted into the distance the carriage has moved by an electronic apparatus located in the control room. An arrow connected to the carriage (see fig. 2.3) traverses a scale fixed to the perspex window of the box. This allows a visual check to be made of the position of the carriage from the CCTV monitoring system. Two limit switches positioned at the ends of the track prevent the carriage being driven against the ends.

Details of the penetrometer carriage are seen in fig. 2.12 and fig. 2.13. The penetrometer is suspended from a gantry through which passes a lead screw . This may be rotated by a permanent magnet DC servo motor mounted on the carriage, so moving the penetrometer up and down. The motor spindle is supported by thrust bearings held by four columns, (fig. 2.13). This assures perfect working under high acceleration (100g). It is possible to vary the rate of penetration by varying the voltage supply to the motor. The electrical signals to the motor are carried by the 'heavy duty' slip rings which can carry currents up to 5 amps. Two columns guide the gantry during radial movement and its position is given by a contact sliding against a potentiometer wire. The gantry is prevented from reaching the fixed ends by an electronic apparatus. This monitors the position of the gantry and turns off the monitor when a limit switch is reached. Electrical signals from the cone load cells, potentiometer wire and cone motor pass along a cable connected between the carriage and a junction box mounted on the hopper.

Following the safety rules for the operation of the Cambridge centrifuge (Schofield, 1980), the new apparatus was proof tested at 125g before being commissioned to be used at 100g.

2.5 Penetrometer probes

Penetrometers Mark II and Mark III (Almeida and Parry,1983) were used in the tests reported here. The Mark I version of the probe (Cheah,1981), was only used for early tests performed in laboratory (see Almeida and Parry, ibid). Penetrometer Mark II, shown in fig. 2.14, has two load cells mounted at the extremities of the penetrometer. Hence independent measurements of point resistance and total load, including side friction, are possible. Initial tests in soft clay showed that load cells of the Mark II probe were producing low signal outputs, which were being affected by electrical noise coming from the slip rings. The outputs from the load cells were increased one hundred times by amplifiers inside the junction box on the centrifuge arm. This reduces the effect of noise produced as the signals pass through the electrical slip rings and on to the control room where they are recorded.

In order to make further improvements to the measurements, the penetrometer Mark III was developed, as shown in fig. 2.15, with a rosette load cell mounted at the top of the penetrometer. An internal rod transmits the tip load to the rosette cell. The four webs of the load cell are subjected to bending and produce signal outputs seven times higher than the load cells of penetrometer Mark II. An additional advantage of the Mark III probe is the smaller diameter than the Mark II probe. However the new design could not accommodate a second load cell to measure total load.

All load cells used in the probes are provided with fully active bridges arranged for temperature compensation and so arranged as to be not affected by bending stresses acting on the probes.

2.6 Hopper apparatus

Following site investigation tests the embankment is constructed in a number of stages by pouring sand from the hopper while the centrifuge is running. The operation of the hopper has been previously described by Davies (1981) and Horner(1981).

The hopper is bolted on to the strong box and the penetrometer apparatus is positioned between the two, as described in section 2.3 (see also fig. 2.2). Front and back views of the hopper are presented in fig. 2.16a, b. The vane apparatus Mark II is bolted to the hopper. The hopper box is divided into 32 separate sand reservoirs which are controlled by cylindrical valve bars indicated in fig. 2.16a. Each bar has drilled holes which coincide with holes at the base of each sand reservoir. To operate the hopper the bars are rotated by a hydraulic jack (see fig. 2.16b) to align the bar holes with the holes on the underside of each reservoir. Due to the short times in which the sand reservoirs are open, ranging from 0.4 s to 1.5 s, double acting solenoid valves are used to operate the air supply to the jack (see fig. 2.16a). The valves are commanded by a timing mechanism located in the control room. The time can be set to open the hopper in steps of 0.1 s.

When the hopper is opened sand particles enter free fall following curvilinear trajectories, fig.2.17, due to the Coriolis effect. This effect occurs when movements take place in the plane of rotation of the centrifuge. Consequently some sand reservoirs close to the liner wall are left empty to prevent sand piling against the wall. Hence the embankment formed inside the hopper is not located in a vertical position above the future position of the embankment, but displaced sideways, as shown in fig. 2.17. The wall of the liner is smooth so that the cross section of the model tested represents half of the prototype envisaged, since the wall of the liner is a plane of symmetry.

2.7 Data acquisition

To sum up briefly, the instrumentation used in the tests described here consisted of: (a) 2 load cells for penetrometer Mark II (1 load cell for penetrometer Mark I); (b) 1 vane load cell; (c) 1 embankment load cell (to be mentioned later); (d) 2 potentiometer displacement transducers (1 for penetrometer and 1 for vane); (e) 1 rotary potentiometer for vane; (f) 1 potentiometer displacement transducer for settlement; (g) 1 optical switch to monitor the position of the carriage; (h) 12 pore pressure transducers, one of them located inside a external reservoir to monitor the water level. In addition to the above, 4 motors were used, 2 for the penetrometer

apparatus and 2 for the vane apparatus. These, together with the instrumentation above, used all the channels of slip rings available.

During centrifuge tests electrical signals from the instrumentation were recorded by a Solartron data logger and by a 14 track Racal tape recorder. Readings from the data logger were produced in punched tape which tranferred to the University IBM 3081 computer to be processed. A set of computer programs was written to help with the processing of the data. These programs were able to transform the raw punched data into engineering results and plot them automatically in suitable scales. Data from the magnetic tape were digitized using an Alpha mini computer and the results were output on a Bryans X-Y plotter. This was to cross check results with the data logger. With the same purpose hand readings of individual channels were taken during the test.

Photographs of the model were taken during flight using a Hasselblad 500 EL/M camera. The camera is mounted above the centrifuge pit and views the package through the perspex window, hence producing photographs equivalent to a cross sectional view of the prototype. A 20 Joule flash synchronized to the centrifuge rotor is triggered by a microswitch attached to the axis of the centrifuge. The duration of the flash is 2 μs. The photographs taken during the test provide a visual record of the model at different stages of a test, as well as allowing measurements to be made of displacements at the boundaries of the model, will be discussed in another report.

3. Vane and penetrometer tests in unloaded clay beds at 100g

3.1 Vane tests

Undrained strengths of Gault and kaolin clays measured with the vane have been obtained from a laboratory testing programme, as shown in fig.3.1 (Almeida and Parry, 1983). It has also been found that kaolin strengths measured with the vane are very close to triaxial strengths reported by Davidson (1980).

Equations used here to predict undrained strengths of the clay cakes prepared for centrifuge tests are

$$\frac{Cu}{\sigma_v'} = 0.22(OCR)^{0.67} \qquad (3.1)$$

for kaolin clay and

$$\frac{Cu}{\sigma_v'} = 0.22(OCR)^{0.76} \qquad (3.2)$$

for Gault clay. The powers in equations 3.1 and 3.2 are the slopes in the diagram of fig.3.1, and 0.22 is the assumed normalized undrained strength for normally consolidated resedimented clay as reported for kaolin (e.g. Mair, 1979).

Equations 3.1 and 3.2 are similar to the equations given by critical state theories. However, equations from experimental data are prefered here since the theoretical equations tend to overestimate undrained strengths, particularly at high OCR, of resedimented clays (Randolph and Wroth, 1981) as well as of natural clays (Almeida, 1982).

All centrifuge tests described in this section and subsequently were carried out at 100g.

The effect of variation of vane rotation rate was observed in clay models MA4 and MA5, as shown in fig. 3.2. It is seen that a fivefold increase of in the rate of rotation from 72°/min to 360°/min produced a variation in the vane strength of some 6% to 10%. Based on experimental and theoretical (Blight,1968) evidence , Almeida and Parry (1983) concluded that 72°/min was an appropriate rate of rotation to be used for tests in kaolin clay.

Vane tests in model SI3, fig.3.3, were performed at a rate of rotation of 72°/min. Tests in models SI3, MA4 and MA5, figs 3.2 and 3.3, show that the undrained strength profile is composed of three distinct parts: a stiff overconsolidated (OCR > 2) top layer 5m thick in the prototype, an intermediate lightly overconsolidated (1 < OCR < 2) layer from 5m to 9 m, and normally consolidated clay below 9m. In fig. 3.3 the profile of design

strengths computed using equations 3.1 and 3.2 is also presented. The agreement between designed and measured strengths is generally good. Vane strengths measured by Davies were considerably higher than design strengths. The reason for this was the cumulative measurement of torques mobilized by blades and shaft, which has been corrected in the Mark II apparatus. One observation which remains unexplained, and was also observed by Davies (1981) is the difference in slopes between measured and predicted strengths in the normally consolidated clay.

3.2 Penetrometer tests

The influence of cone penetration rates was studied in clay models SI3 and MA5 and results are presented in fig. 3.4 and fig.3.5, respectively. It is apparent that variations of the rate of penetration between 2 and 20 mm/s have little effect on q_c. A reversal of the effect is shown with increasing overconsolidation. Thus in flight penetrometer tests confirm results in the laboratory reported by Almeida and Parry (1983). The rate of penetration used in subsequent tests reported here is 5mm/s unless otherwise stated. This rate of penetration is convenient for recording of data during centrifuge test.

Penetrometer tests in model SI3 were performed with the Mark II probe whereas in model MA5 tests were performed with the Mark III probe. Differences in magnitudes of q_c between tests SI3 and MA5 can probably be attributed to different details in the geometry of the cone tips.

Clay model MA5 was used to assess factors such as influence of the radial penetration of the cone probe and homogeneity of the clay sample. Penetrometer tests C1 and C4 were performed at a location 18 mm from the outside boundaries of the strong box, at left and right hand sides, respectively. Penetrometer test C3 was performed at the centre line of the clay sample. Results of the three tests in clay sample MA5, fig. 3.6, are quite close. Therefore, as far as point resistances are concerned it is not important whether the penetrometer is driven perpendicular to the clay cake surface (on its centre) or slightly inclined to the clay surface, in the direction of the gravity field away from the centre. It must be noted that since the lower normally consolidated layer is subjected to radial

consolidation, results of penetrometer tests in the direction of the gravity field in any position across the box should be very close.

Clay models MA4, MA5 and MA6 were used for centrifuge modelling of embankment construction. Results of penetrometer tests performed immediately before placing the embankment, using the Mark III probe, fig. 3.7, illustrate the achieved repeatability of clay cakes, as well as the consistency of the site investigation technique. Penetrometer tests in clay model MA3, also used for embankment modelling, are presented in the next section.

3.3 Correlation between vane and penetrometer tests

Both vane and penetrometer tests were performed during centrifuge testing of clay models SI3, MA4 and MA5. Penetration tests were performed at a rate of 5mm/s, and vane tests at a rate of rotation of 72°/min for tests SI3 and MA4 and at a rate of 360°/min for test MA5. Results of vane and penetrometer tests are compared in figs. 3.8, 3.9 and 3.10 for models SI3, MA4 and MA5 respectively. Profiles with depth of q_c and c_u, the values of which are also presented in table 3.1, are similar in shape, but values of q_c are considerably lower than expected, as discussed below. Results of vane and penetrometer tests are usually correlated using equations.

$$N_k = \frac{q_c}{c_u} \tag{3.3}$$

or

$$N_c = \frac{q_c - \sigma_v}{c_u} \tag{3.4}$$

Computations of N_k and N_c for tests SI3, MA4 and MA5 are shown in table 3.1. It should be noted that:

a) Values of N_k vary between 8 and 13 for tests in clay models MA4 and MA5 whereas values obtained in laboratory tests (Almeida and Parry, 1983) ranged between 14 and 15 for Gault clay and between 9 and 11 for kaolin;

b) Values of N_c decrease with depth (or with decreasing OCR) which is consistent with patterns obtained by Almeida and Parry (1983) and Francescon (1980) for tests in laboratory, as seen in fig. 3.11. However, centrifuge values are unexpectedly low at large depths (OCR = 1), with some negative values in test MA5, as seen in table 3.1;

The higher values of N_c and N_k measured in the laboratory compared with the centrifuge may be explained in part by the different boundary conditions. In laboratory tests the restriction on displacements imposed by the consolidometer piston during cone penetration is quite different from the centrifuge where the soil displaced by the penetrometer can move to the surface. This aspect may be important for point resistances at shallow depths.

The second possible reason, affecting more strongly point resistances measured at greater depths, is the pore pressure effect associated with the geometry of the cone tip, as explained below.

During penetration, downward pressure acting on the recessed top of the cone tip decreases measured point resistances, as shown in fig.3.12. This may be direct pore pressure or pressure from the flexible seal caused by the pore pressure acting on it. This problem, which affects in varying degrees all existing designs of cones, has been pointed out by Baligh et al. (1981) and Campanella and Robertson (1981). If uniform pore pressure u acts around the tip, the true point resistances would be given by

$$q_T = q_c + (1 - a)u \qquad (3.5)$$

where a is the net area ratio of the core tip as defined in fig. 3.12. For penetrometer Mark II a = 0.64 and for penetrometer Mark III a = 0.39. [1]

---

[1] For the Fugro cone a=0.45 (De Ruiter,1982) and for the piezocone used by Almeida and Parry(1983), a=0.50.

The pore pressure u is given by

$$u = u_o + \Delta u \tag{3.6}$$

where u_o is the hydrostatic pore pressure and Δu is the excess of pore pressure developed during penetration. Piezocone measurements have not been made in the centrifuge, but Almeida and Parry (1983) have obtained $\Delta u/q_c$ of about 1.0 when testing Gault clay in laboratory. It was found that this ratio decreased only slightly with the OCR. However, for obvious reasons, a more fundamental pore pressure ratio is $\Delta u/q_T$. Assuming uniform pore pressure around the tip, the value of $\Delta u/q_T$ corresponding to $\Delta u/q_c$ obtained by Almeida and Parry(ibid) is 0.67. This compares with $\Delta u/q_T$=0.6 found by Campanella et al(1983) for a deltaic soil. Baligh et al(1981) prefer to use u/q_T which was found to be equal to 0.85 for the Boston Blue clay.

Substituting $\Delta u = 0.67 q_T$ into eq. 3.6 and eq. 3.6 into eq. 3.5, values of q_T can be found, as shown in table 3.1 for tests SI3, MA4 and MA5. Corresponding values of N_{cT} and N_{kT} computed from q_T are also given in table 3.1 and it is seen that all values have increased considerably. Values of N_{cT} for centrifuge test SI3 are shown in fig. 3.13 together with values found in the laboratory for kaolin (Almeida and Parry,1983). In both sets of tests the same probe Mark II was used. As observed in fig. 3.13, the agreement between values of N_{cT} obtained in laboratory and during centrifuge flight is satisfactory.The discrepancy between laboratory and centrifuge values probably arises from the assumption of uniform pore pressure around the tip. Future studies of the pore pressure distribution should lead to even closer agreement between the values.

4. Penetrometer tests during embankment construction

4.1 Embankment construction

The loading sequence used for embankment construction during centrifuge test MA3 [2] is shown in fig.4.1 and Table 4.1, where times for model construction (t_m) and corresponding times at prototype scale (t_p) are indicated. When migration and dissipation of pore pressures occur during static events in centrifuge tests, model and prototype times are related by $t_p=n^2t_p$, where n is the centrifuge acceleration (in g), as the drainage path in the model is n times shorter than in the prototype. Therefore one hour of centrifuge flight corresponds to about one year at prototype scale. This shortening of time is obviously a great advantage of centrifuge tests.

The embankment was loaded in five lifts, fig.4.1, the last two lifts being applied in quick succession, failure occurring shortly after lift 5 was poured, at a height of 123mm (12.3m). The height of failure for instantaneous loading of the embankment for undrained conditions would have been about 60 mm (6 m). Embankment geometries at the end of stages 2, 3, 4 and 5 (before failure) are shown in fig.4.2. It is seen that the foundation experienced considerable distortion during embankment construction. Analysis of the foundation behaviour under the embankment will be the subject of another report.

Embankment densities vary for each lift due to factors such as time of hopper opening and amount of sand available in the hopper. It is possible to estimate the average density of the embankment at the end of the test by computing weight and volume of sand used. The average density measured was 16.3 KN/m^3 which corresponds to a voids ratio of 0.595 and a relative density of 78%, for the 30/52 Leighton Buzzard sand.

A load cell was placed on the top of the foundation to measure the length of construction time. The load cell could not give reliable

---

[2] Vane strengths measured in clay model MA4 (see fig.3.2) are representatives of clay model MA3.

information about embankment pressures, as discussed by Davies(1981).

4.2 Penetrometer tests

During centrifuge testing of clay model MA3, seven cone penetration tests were performed as follows: cone tests C1 and C2 before lift 1 was poured, cone test C3 during stage 2 and cone tests C4, C5, C6 and C7 during stage 3. Times in which tests were performed are presented in table 4.2. The position of each cone test together with the geometry of the embankment for each stage are presented schematically in fig.4.3 where the foundation is shown undeformed for sake of simplicity.

Results of cone penetration tests during stage 3 are presented in fig. 4.4. The penetrometer is pushed through the embankment to reach the soft clay underneath. Measured cone resistances in the sand embankment are much larger than in the clay foundation. Important points to be raised regarding measured penetration resistances in the sand embankment are:

(a) q_c reaches a maximum value, after which it decreases as the soft clay foundation underneath is approached; that is because as the cone tip approaches the soft clay, punching failure occurs, as explained by Meyerhoff and Sastry (1978). The shape of the penetration curve is consistent with results presented by the authors for dense sand overlying soft clay.

(b) q_c max increases as the thickness of the sand embankment increases, which is also consistent with the equation proposed by Meyerhoff & Sastry (1978). Punching coefficients backfigured from the results presented here are smaller than the theoretical ones proposed by the above authors. However, a strict comparison is not possible since most of the tests at fig.4.4 were performed in the embankment slope.

The important point to be raised from fig.4.4 regarding the clay foundation is that q_c increases for tests performed towards the centre line of the embankment as a result of larger surcharges causing more consolidation of the embankment, hence larger q_c. This trend is better

appreciated in fig.4.5 where point resistances of the clay foundation under lift 3 are plotted in enlarged scale. Point resistances at the top of the soft clay close to the embankment are higher than expected. These values might not be very reliable because as the cone tip approaches the soft clay, failure is occurring by punching of a cylindrical mass of strong soil under the tip into the soft clay.

Cone penetration test C3 performed during lift 2 at a position close to cone penetration test C7 performed during lift 3 is presented in fig. 4.6, together with penetration test C1 of the virgin foundation. It is clear that a substantial gain of resistance is experienced by the clay foundation in the course of the construction of the embankment in stages.

Analysis of the gain of strength from embankment construction and undrained strength profiles deduced from the point resistances will be the subject of another report.

5. Summary and conclusions

In order to measure clay strength during centrifuge flight, miniature vane and penetrometer apparatuses have been developed.

Apparatuses and experimental procedure used to prepare clay samples for centrifuge tests of embankments on soft clay are described. A bed consisting of Gault clay overlying kaolin clay is consolidated from slurry. In order to produce a stiff crust at the top, the clay sample is subsequently subjected to a partial consolidation in the laboratory with drainage at the top only. When the stress history is completed after a long consolidation run during centrifuge flight (100 g), the clay sample consists of a 160 mm (16 m) soft clay foundation of which the top 90 mm (9 m) layer is over consolidated and the bottom 70 mm (7 m) layer is normally consolidated.

The vane apparatus Mark II developed to perform vane tests in flight is described and the improvements over the old version are detailed. In flight vane strengths showed that a stiff crust 50 mm (5 m) thick is obtained as a result of the induced stress history. Results obtained with

vane Mark II compare well with predicted strengths. A new penetrometer apparatus capable of moving to different positions in plan during a centrifuge test is described in detail. Studies on the influence of the rate of penetration show that variations between 2 and 20 mm/s have little effect on q_c, which confirms observations in the laboratory reported by Almeida and Parry (1983).

Curves of penetration resistance with depth are similar in shape to curves of vane strength with depth, hence the stiffer layer obtained as a result of the stress history is indicated in both tests. However, measured point resistances are low and consequently values of N_c are lower than expected. The main reason for this seems to be related to the high pore pressures developed during penetration associated with the geometry of the cone tip, causing a decrease in the measured point resistance. Modified point resistances q_T assuming a uniform distribution of pore pressure around the cone tip during penetration have produced considerably higher N_{cT}. However, because pore pressure distributions developed during cone penetration are unknown, no definite conclusions could be obtained. Consequently, more work on the performance of miniature cone penetrometers and correlations with vane tests, are needed.

The loading sequence during construction in stages of an embankment in flight and results of penetrometer tests performed before and after placing the embankment are presented. Resulting penetration curves obtained when the penetrometer is pushed through the embankment into the soft clay are consistent with findings obtained by Meyerhoff and Sastry (1978). Penetrometer tests performed at various locations under the embankment show that point resistances increase for tests performed towards the centre line of the embankment. The gain of resistance of the foundation due to consolidation of the soft clay in the course of construction of the embankment in stages is also clearly illustrated.

Acknowledgements

The authors are grateful to Mr P W Turner for assistance in developing the penetrometer equipament and to Dr R G James for assistance during the centrifuge tests.

References

Almeida, M. S. S. (1982) The undrained behaviour of the Rio de Janeiro clay in the light of critical state theories. Technical Report, Cambridge University, CUED/D - SOILS TR 119(1982)

Almeida, M.S.S. and Parry, R.H.G. (1983) Tests with centrifuge vane and penetrometer in a normal gravity field, Cambridge University, CUED/D-SOILS TR141(1983).

Baligh, M. M., Assouz, A. M., Wissa, A. Z. E., Martin, R. T. and Morrisson, M.J. (1981) The piezocone penetrometer. Proc. ASCE Conf. on Cone Penetration Testing and Experience, St Louis, Missouri, October 1981.

Blight, G.E. (1968) A note on field vane testing of silty soils. Canadian Geot. Jour., 5, No.3, 142-149.

Campanella, R.G. and Robertson, P.K. (1981) Applied cone research. ASCE Proc. of Cone Penetration Testing and Experience, St Louis, Missouri, October 1981, pp.343-362.

Campanella, R. G., Robertson, P. K. and Gillespie, D.(1983) Cone penetration testing in deltaic soils. Can. Geot. Jour., Vol. 20, pp 23-35.

Cheah, H. (1981) Site investigation techniques for laboratory soil models. M.Phil. Thesis, Cambridge University Engineering Department, England.

Davidson, C.S. (1980) The shear modulus of clays. Part II Research Report, Cambridge University Engineering Department, England.

Davies, M.C.R. (1981) Centrifugal modelling of embankments

on clay foundations. Ph.D. Thesis, Cambridge University Engineering Department, England.

Davies, M.C.R. and Parry R.H.G. (1982) Determining the shear strength of clay cakes in the centrifuge using a vane. Geotechnique, 32, No.1, 59-62.

De Ruiter, J. (1982) The static cone penetration test. State-of-the-art report. Proc. of the II ESOPT, 389-405, Amsterdam.

Francescon, M. (1983) Model pile tests in clay. Ph.D. Thesis, Cambridge University Engineering Department, England.

Horner, J. N. (1982) Centrifugal modelling of multilayer clay foundations subjected to embankment loading. PhD thesis, King's College, University of London.

Mair, R.J. (1979) Centrifugal modelling of tunnel construction in soft clay. PhD thesis, Cambridge University Engineering Department, England.

Meyerhoff, G.G. and Sastry, V.V.R.N. (1978) Bearing capacity of piles in layered soils. Part 2. Sand overlying clay. Can. Geot. Jour., 15(2), pp. 183-189

Schofield, A.N. (1980) 'Cambridge geotechnical centrifuge operations'. Geotechnique, Vol.30(3), 227-268.

Randolph, M.F. and Wroth, C.P. (1981) Application of the failure state in undrained simple shear to the shaft capacity of driven piles. Geotechnique 31, No 1, 143-157

TABLE 3.1 - Correlation between vane and penetrometer tests

Clay model	depth (mm)	σ_v (kPa)	c_u (kPa)	q_c (kPa)	N_k	N_c	q_T (3) (kPa)	N_{kT}	N_{cT}
SI3 (1)	13	38	14.7	174	11.8	9.2	239	16.3	13.7
	32	66	12.9	150	11.5	6.4	217	16.8	11.7
	51	96	9.4	142	14.5	4.3	215	22.9	12.7
	70	126	10	160	15.8	3.4	248	24.5	12.0
	89	155	11	182	15.8	2.8	286	24.0	11.0
	108	184	16.0	218	13.8	2.3	342	21.0	9.9
	127	214	20.3	253	12.6	2.0	397	20.0	9.0
	144	240	24.5	282	11.8	2.0	443.5	8.3	8.3
MA4 (2)	13	38	14.2	118	8.3	5.7	223	15.7	13.0
	33	69	11.6	115	9.9	4.0	238	20.6	14.6
	53	98	9.0	108	12.0	1.1	247	27.5	16.6
	79	138	10.9	140	12.8	0.2	328	30.1	17.5
	93	160	12.7	162	12.8	0.8	380	30.0	17.3
	120	204	20.9	205	9.9	0.1	480	23.0	13.2
	147	245	29.7	265	8.9	0.7	610	20.5	12.3
MA5 (2)	13	38	14.0	130	9.3	6.6	243	17.4	14.7
	33	69	10.4	115	11.0	4.4	238	22.9	16.3
	53	98	10.0	105	10.5	0.7	242	24.0	14.4
	73	130	10.5	120	11.4	<0	288	27.4	15.1
	93	160	14.0	145	10.4	<0	351	25.0	13.7
	120	204	23.0	190	8.3	<0	455	19.8	10.9
	147	254	31.5	232	7.4	<0	554	17.6	9.8

NOTES:

(1) penetrometer Mark II was used

(2) penetrometer Mark III was used

(3) q_T assuming $\Delta u = 0.67\ q_T$ in eq. 3.5

TABLE 4.1 - Details of the embankment construction - model MA3

lift. no.	embankment height, mm	time for construction	
		model (min)	prototype (days)
1	30 (3.0)(1)	0	0
2	54 (5.4)	34	236
3	83 (8.3)	132	916
4	98 (9.8)	255	1770
5	123 (12.3)	255.5	1774

(1) embankment height in prototype scale (m)

TABLE 4.2 - Penetrometer tests

Test	Event	time(1) (min)
C1	before lift 1	-90
C2	before lift 1	-45
C3	during stage 2	116
C4	during stage 3	223
C5	during stage 3	228
C6	during stage 3	235
C7	during stage 3	240

(1) zero time corresponds to the time of the start of embankment construction (lift 1)

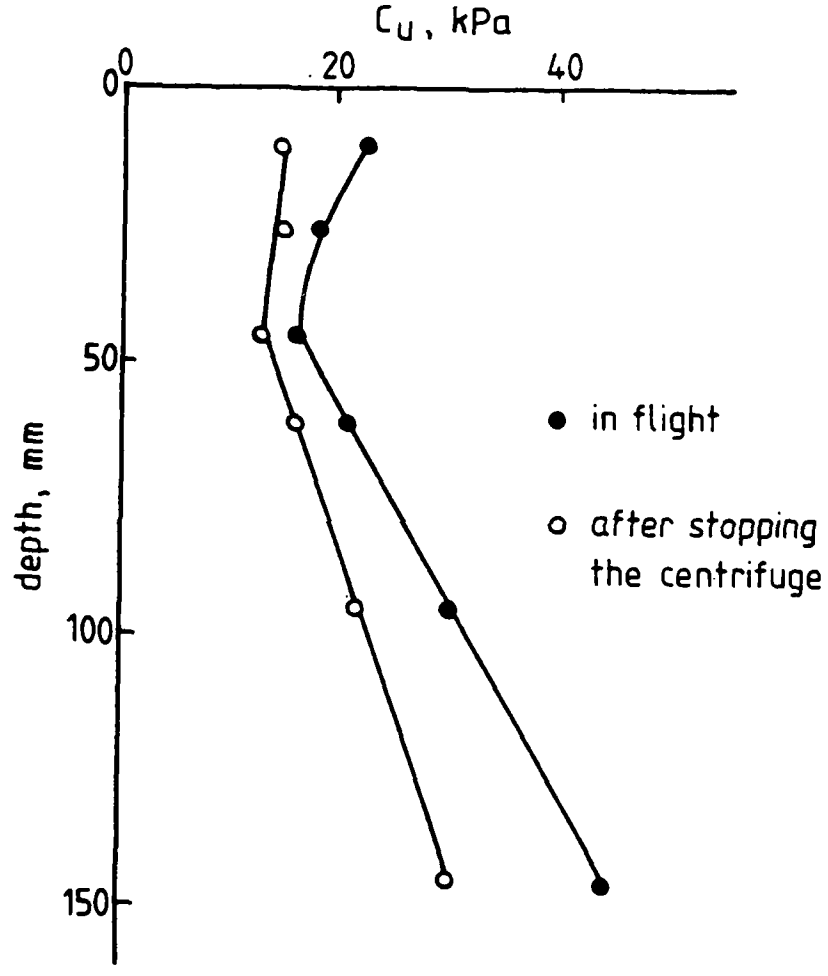

Fig. 1.1 - Vane strength measured in flight and after stopping the centrifuge (test MA1)

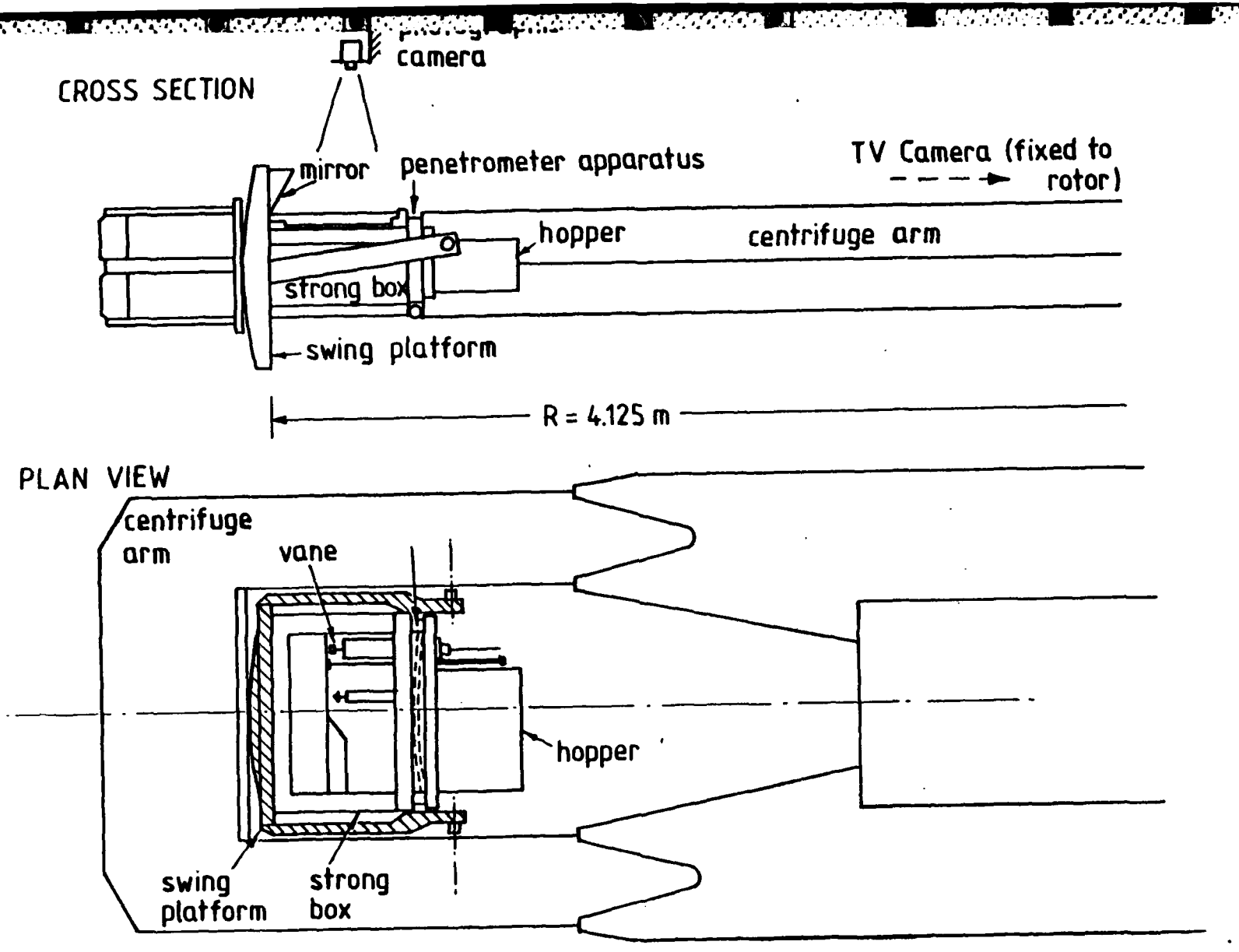

Fig. 2.1 - Package mounted to the centrifuge

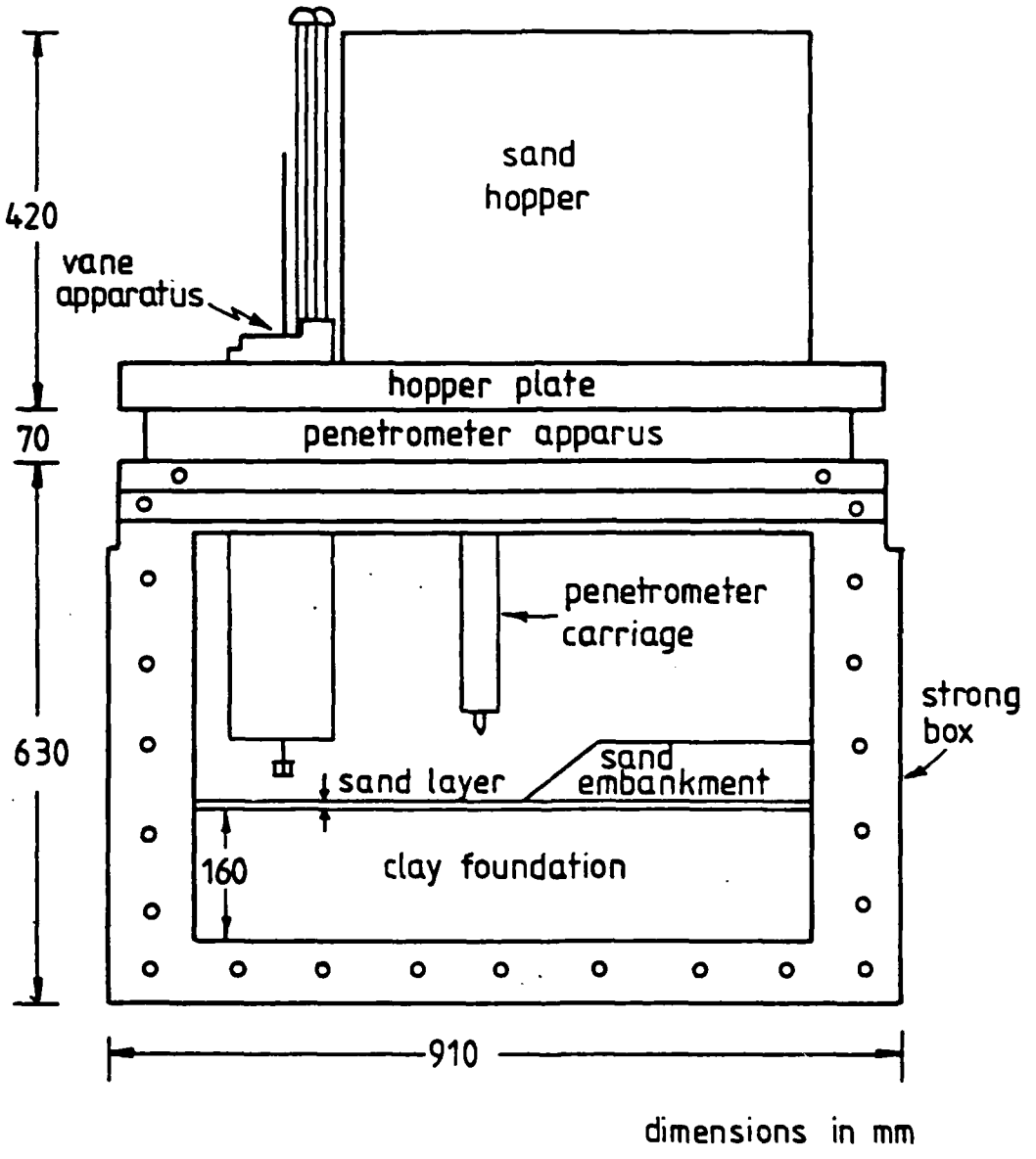

Fig. 2.2 - Package for centrifuge test

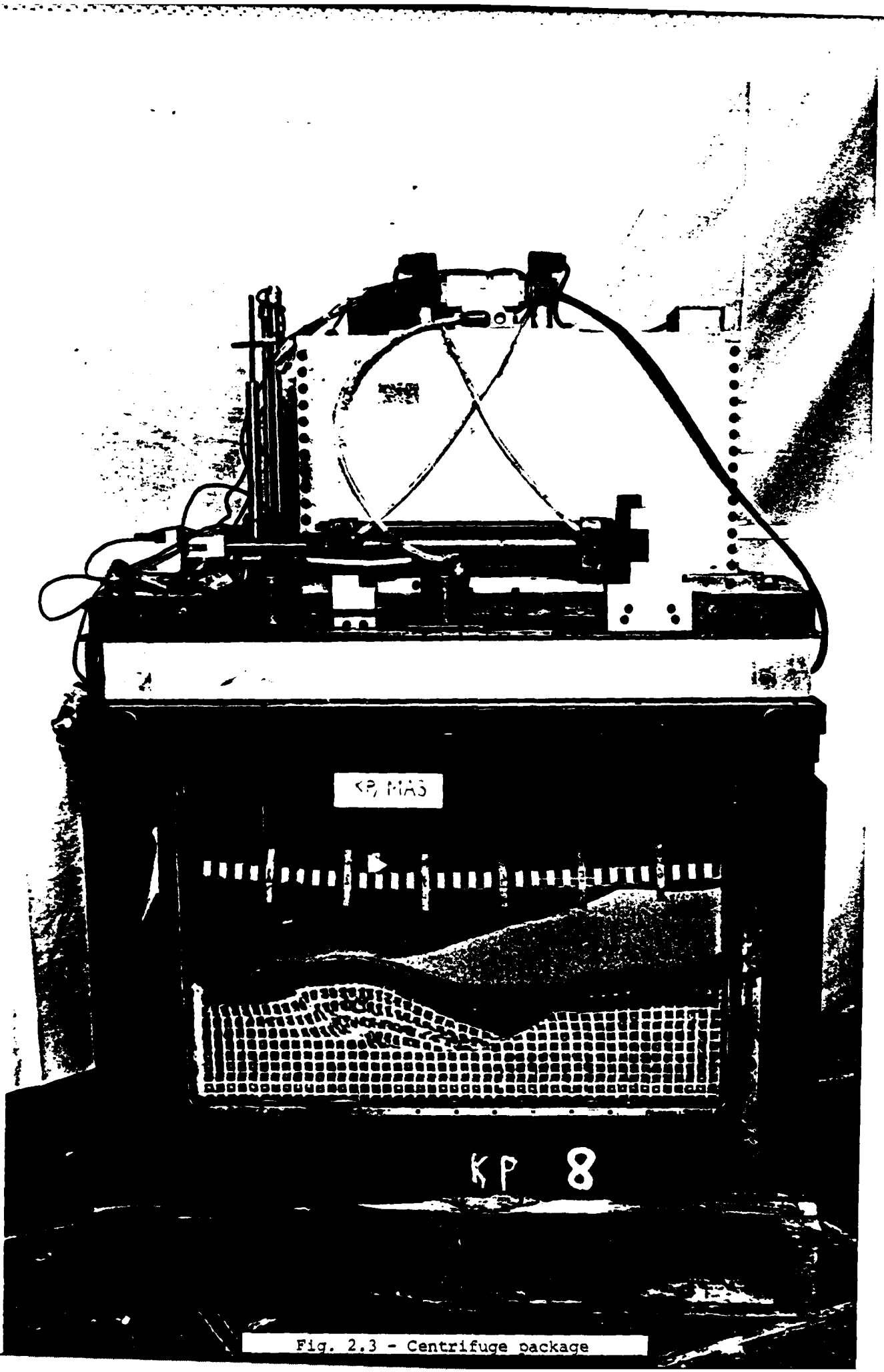

Fig. 2.3 - Centrifuge package

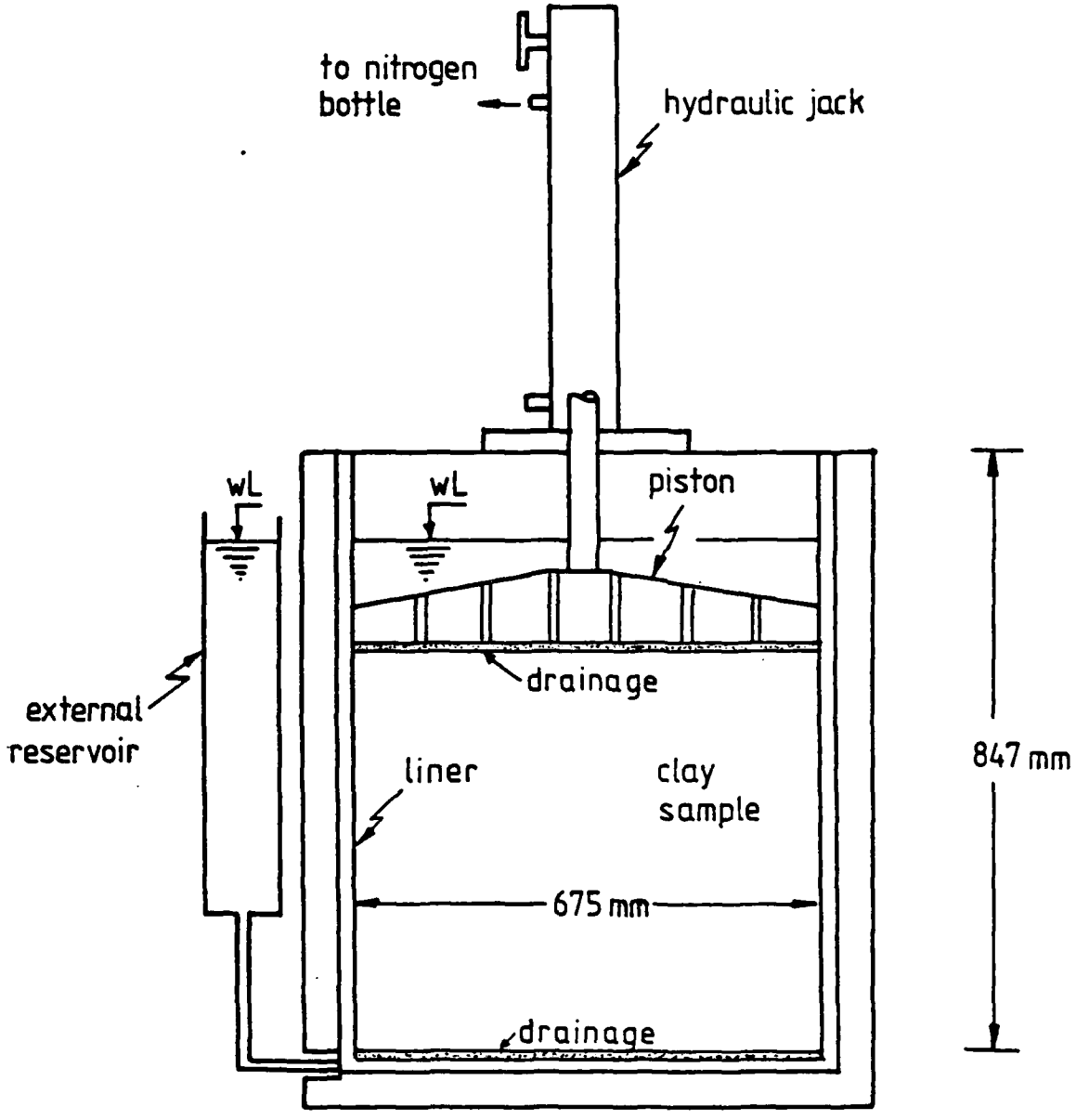

Fig. 2.4 - Cross section of the consolidometer

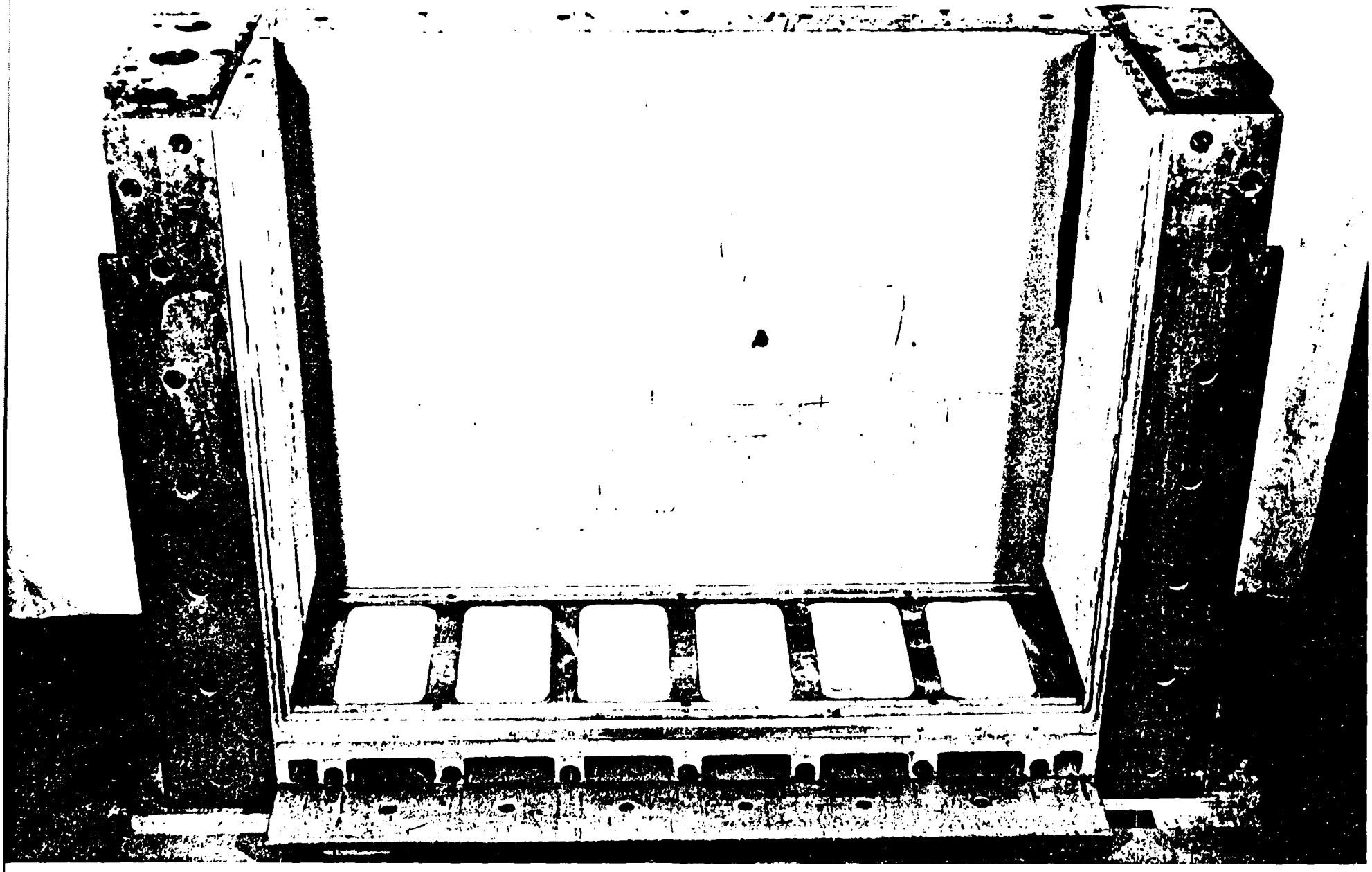

Fig. 2.5 — Strong box and liner

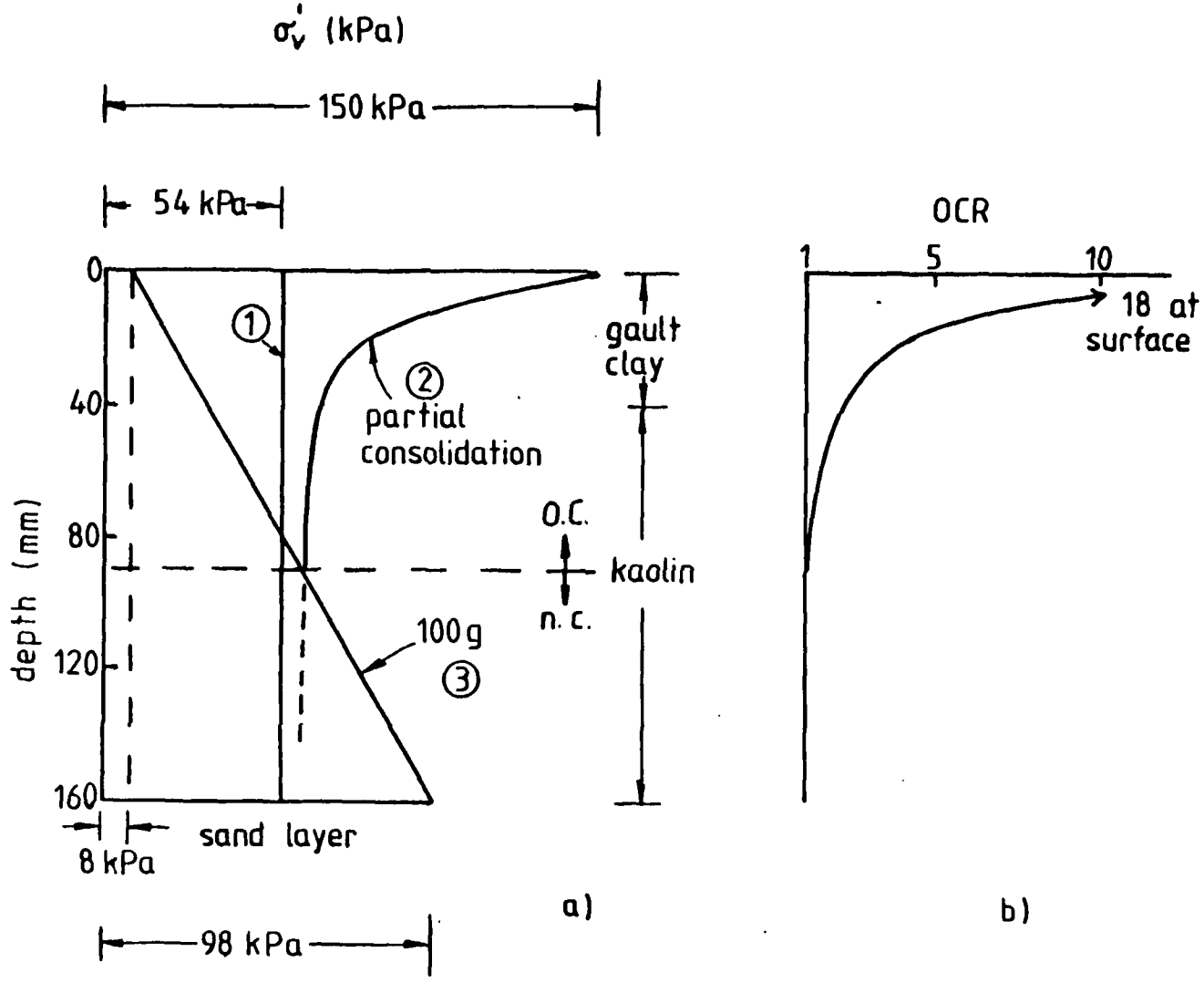

Fig. 2.6 - Stress history for clay models

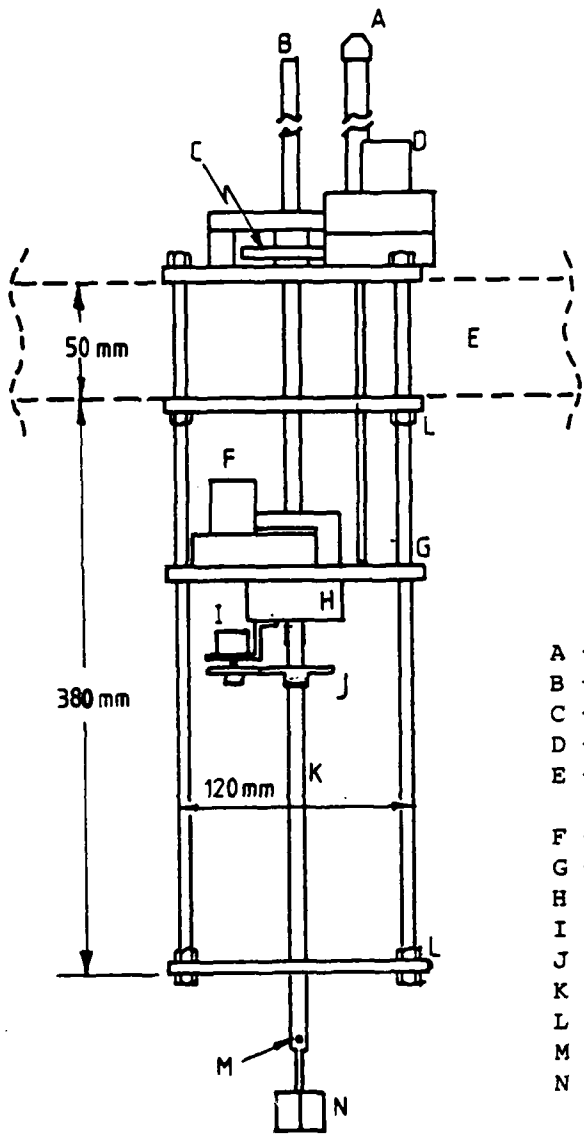

A - displacement transducer
B - threaded rod
C - gearing system
D - vertical driving motor
E - adjustable space to suit supporting device
F - torque motor
G - moving platform
H - bearing block
I - rotary potentiometer
J - nylon gears
K - shaft
L - spacing plate
M - slip coupling
N - vane blades (18 mm dia. × 14 mm high)

Fig. 2.7 - Vane apparatus Mark II

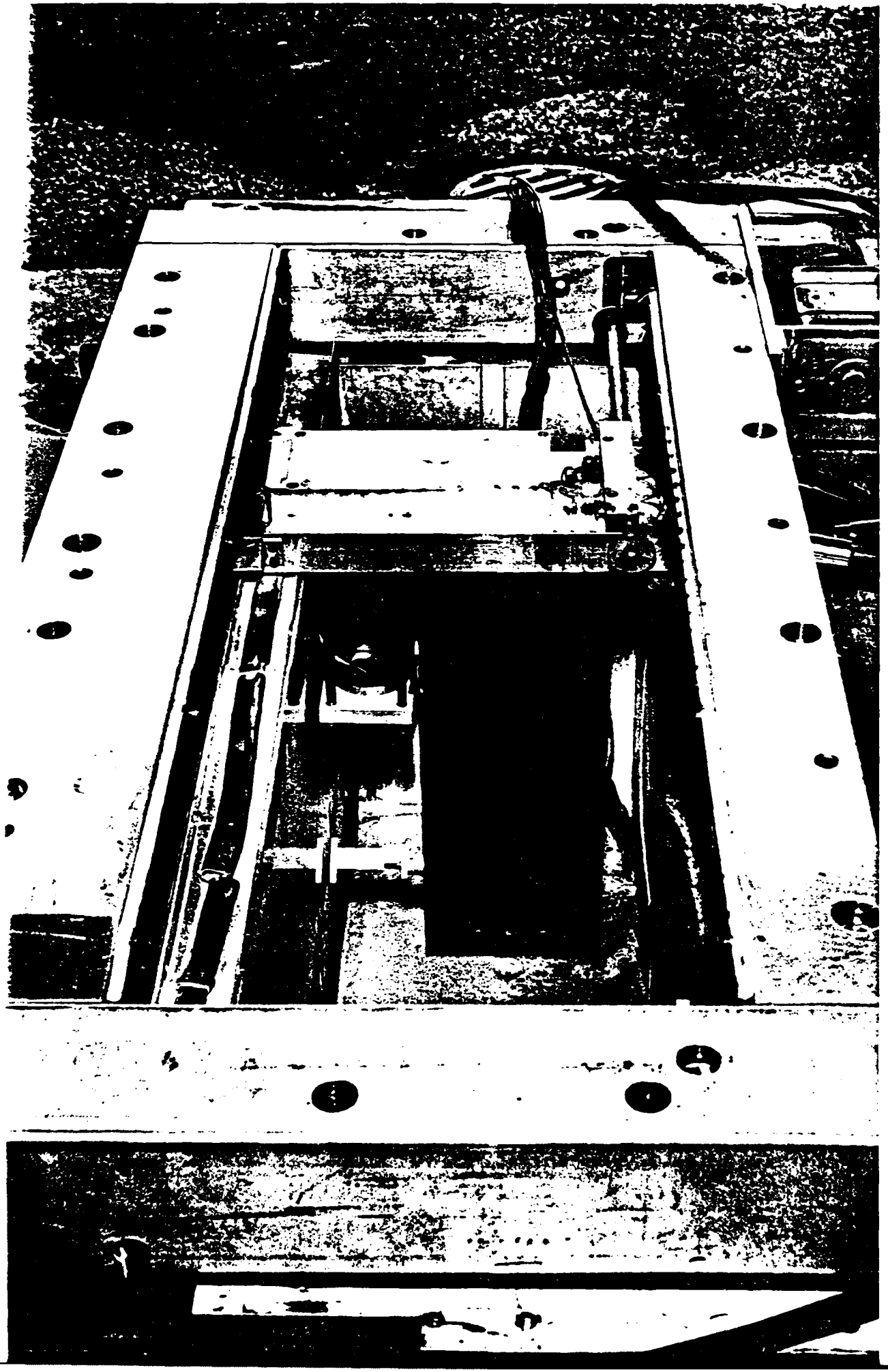

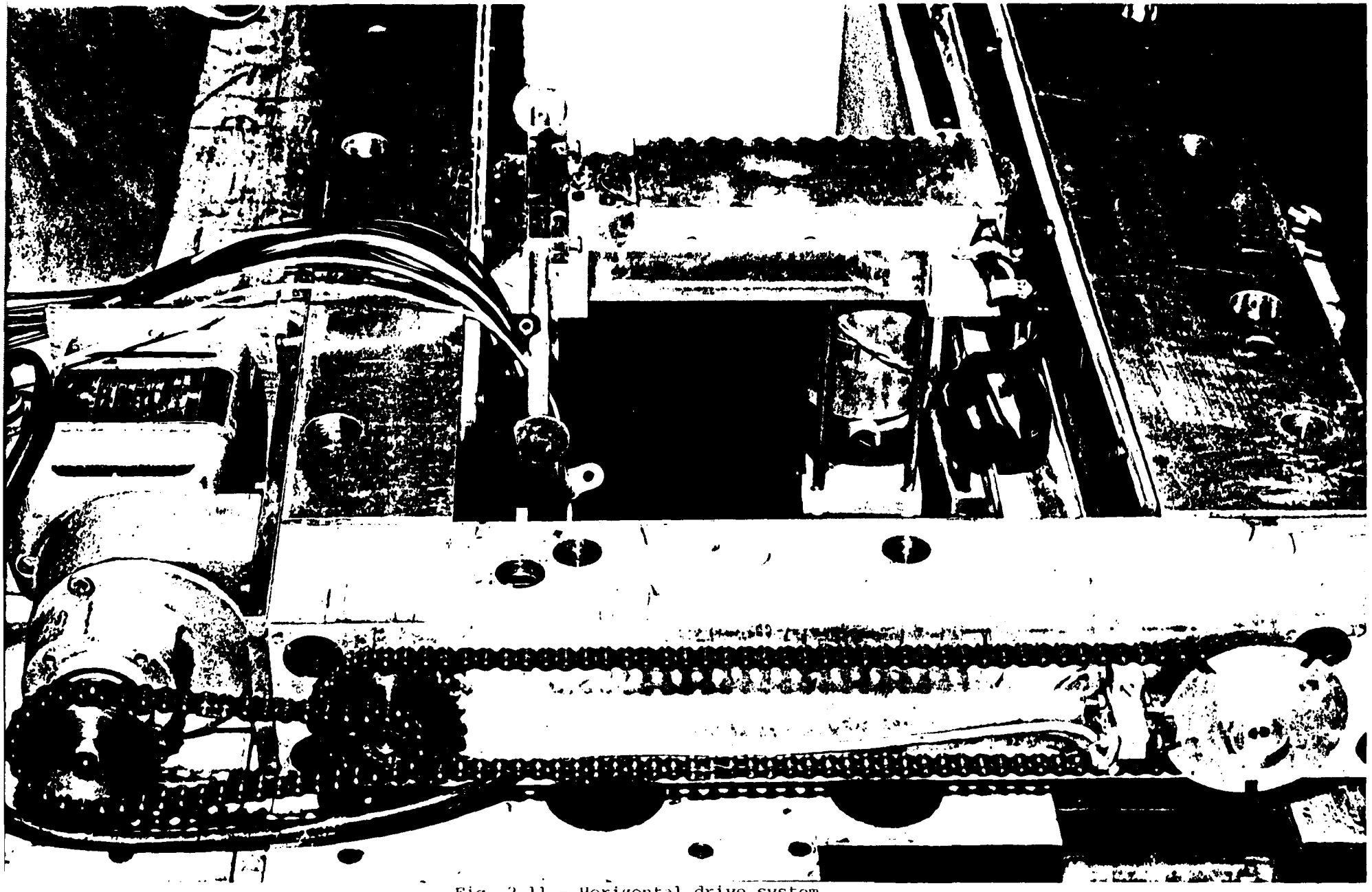

Fig. 2.11 - Horizontal drive system

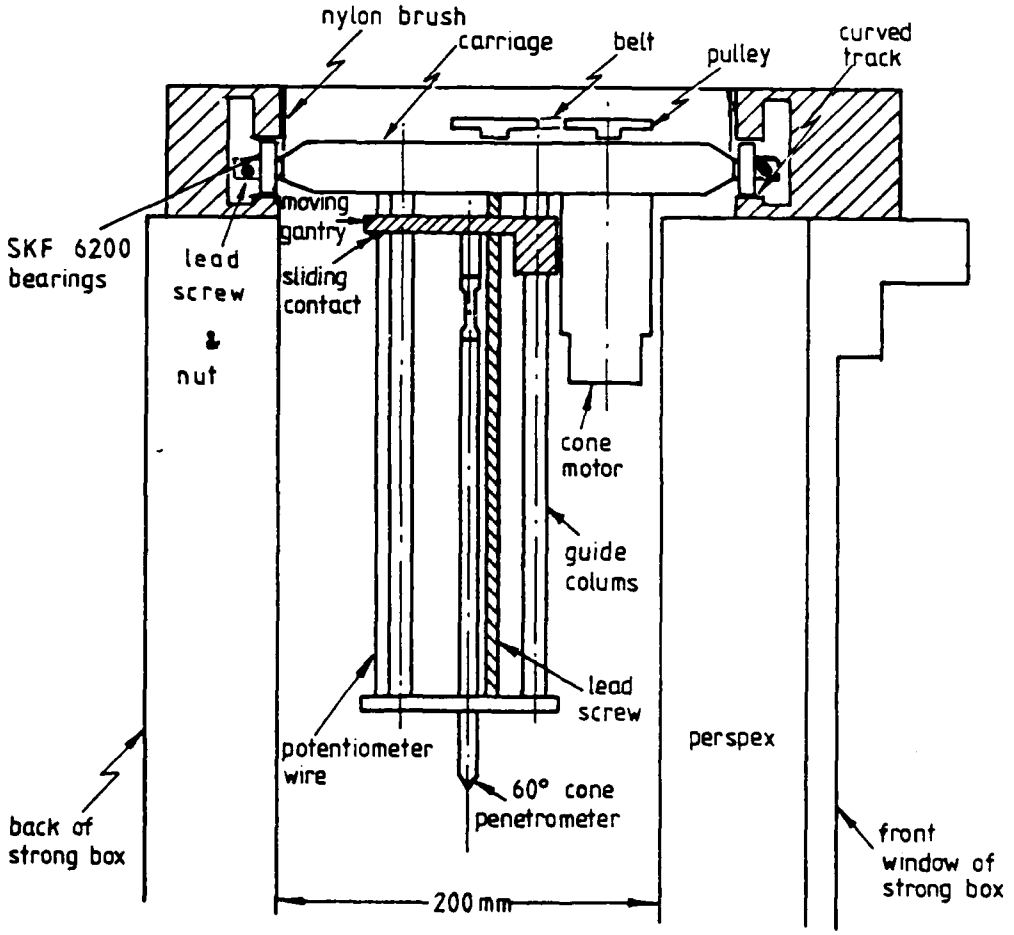

Fig. 2.12 - Details of carriage

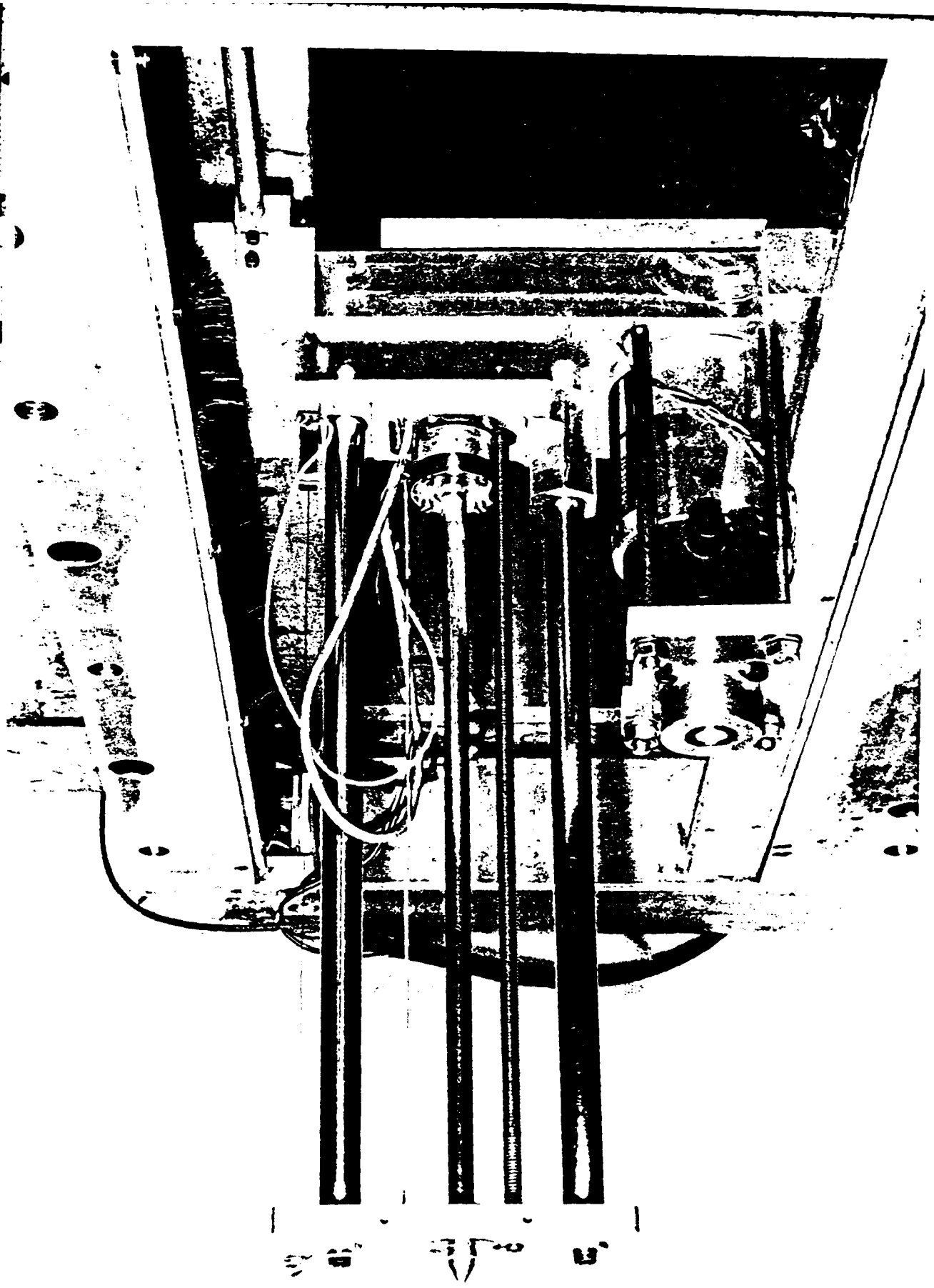

Fig. 2.13 - Carriage and penetrometer

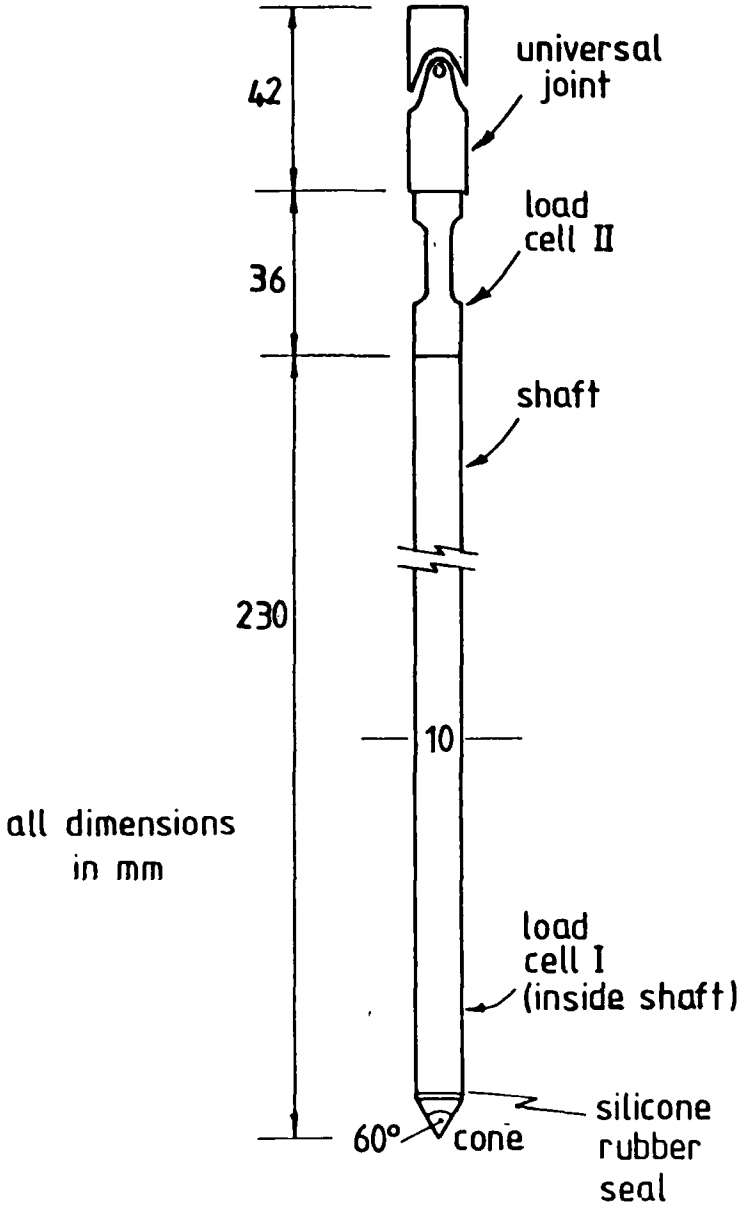

Fig. 2.14 - Penetrometer Mark II

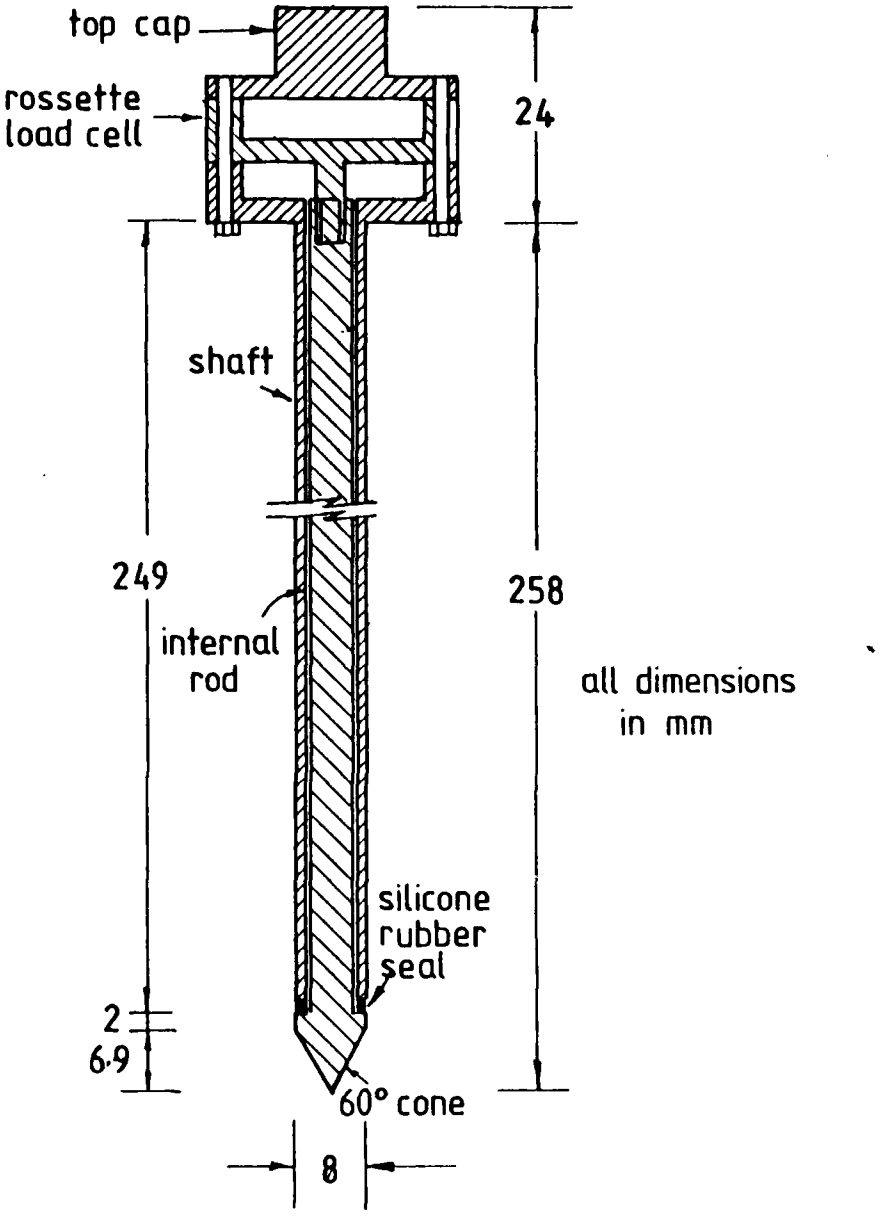

Fig. 2.15 - Penetrometer Mark III

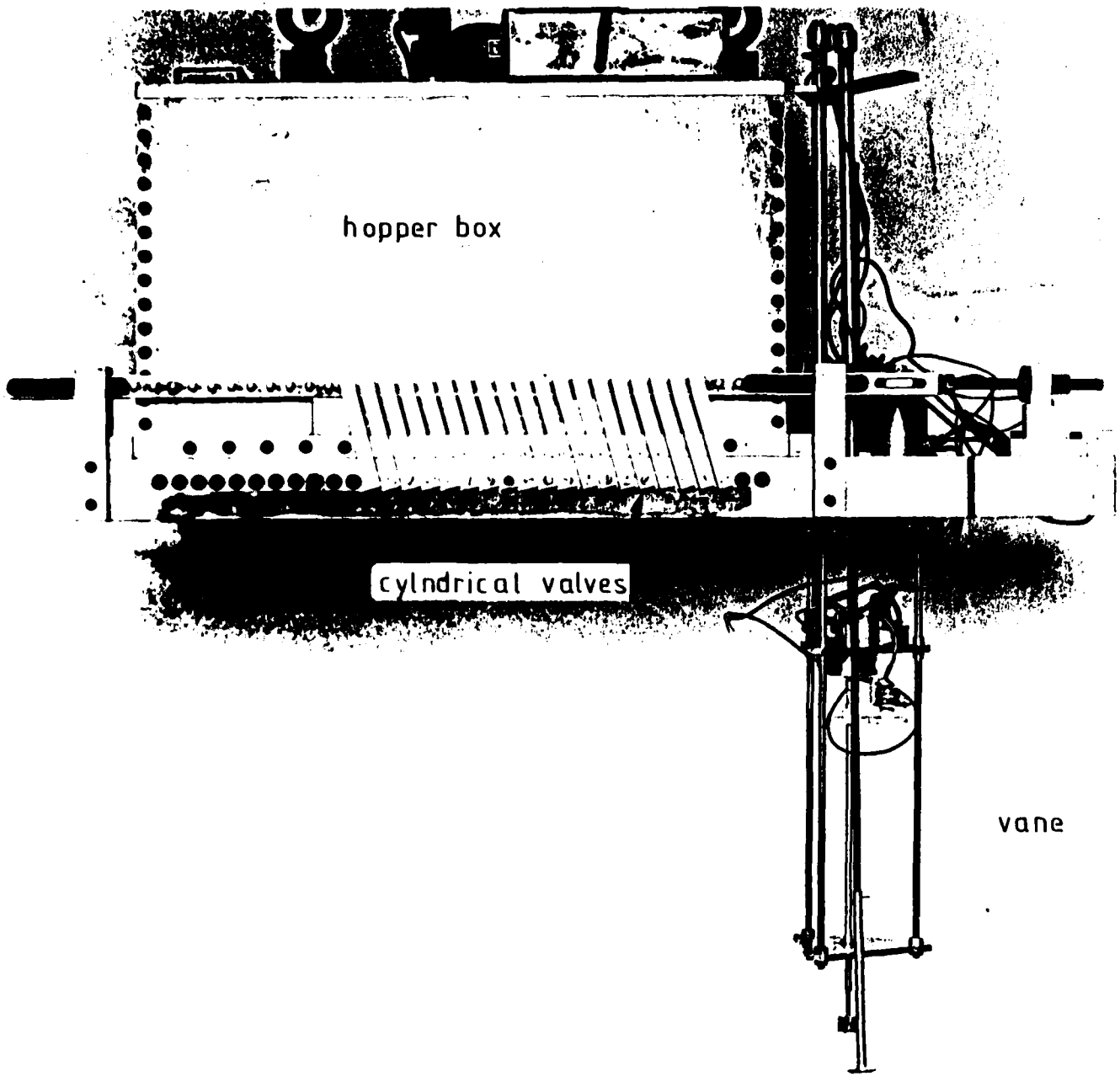

Fig. 2.16a - Back view of the hopper

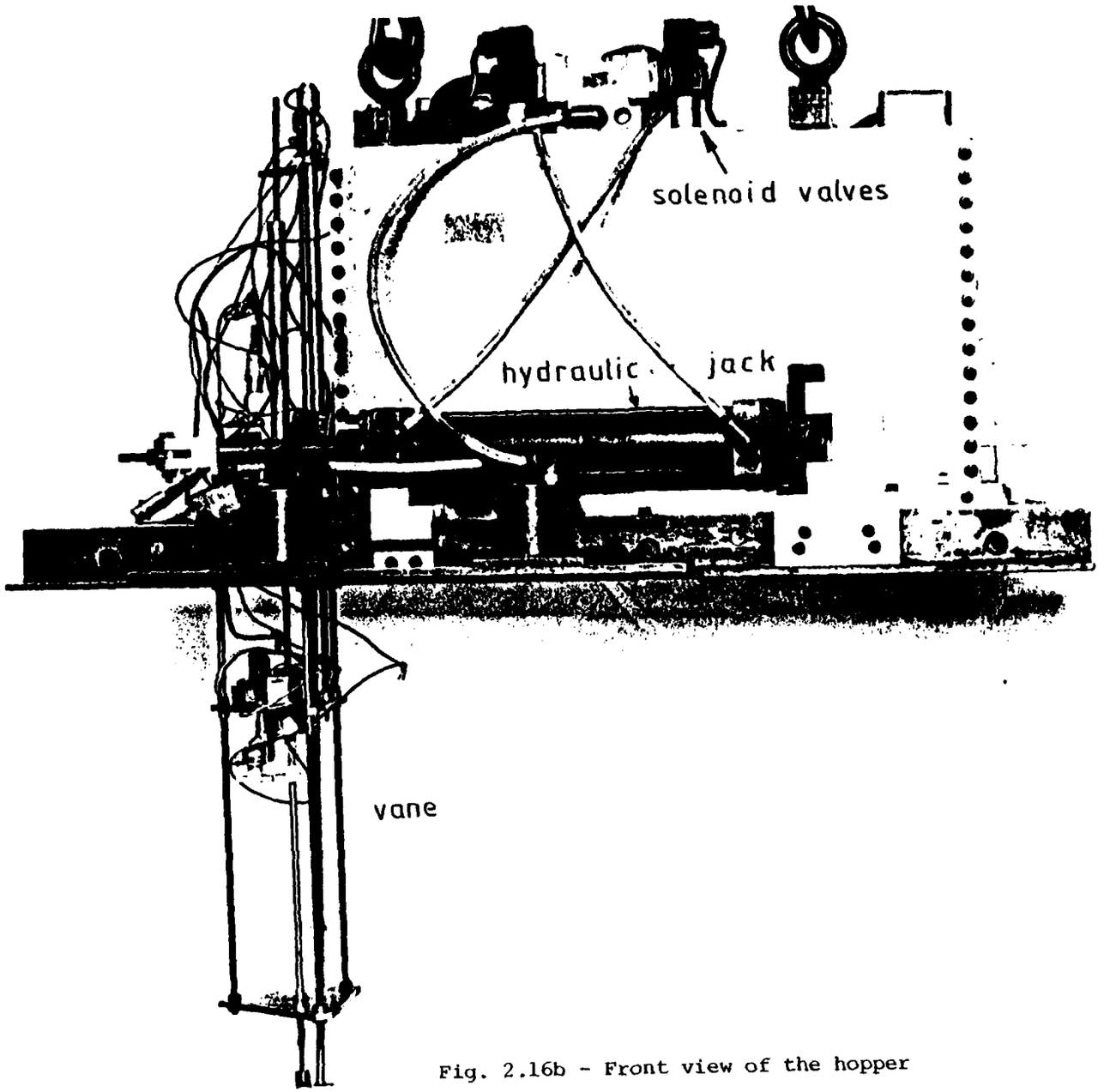

Fig. 2.16b - Front view of the hopper

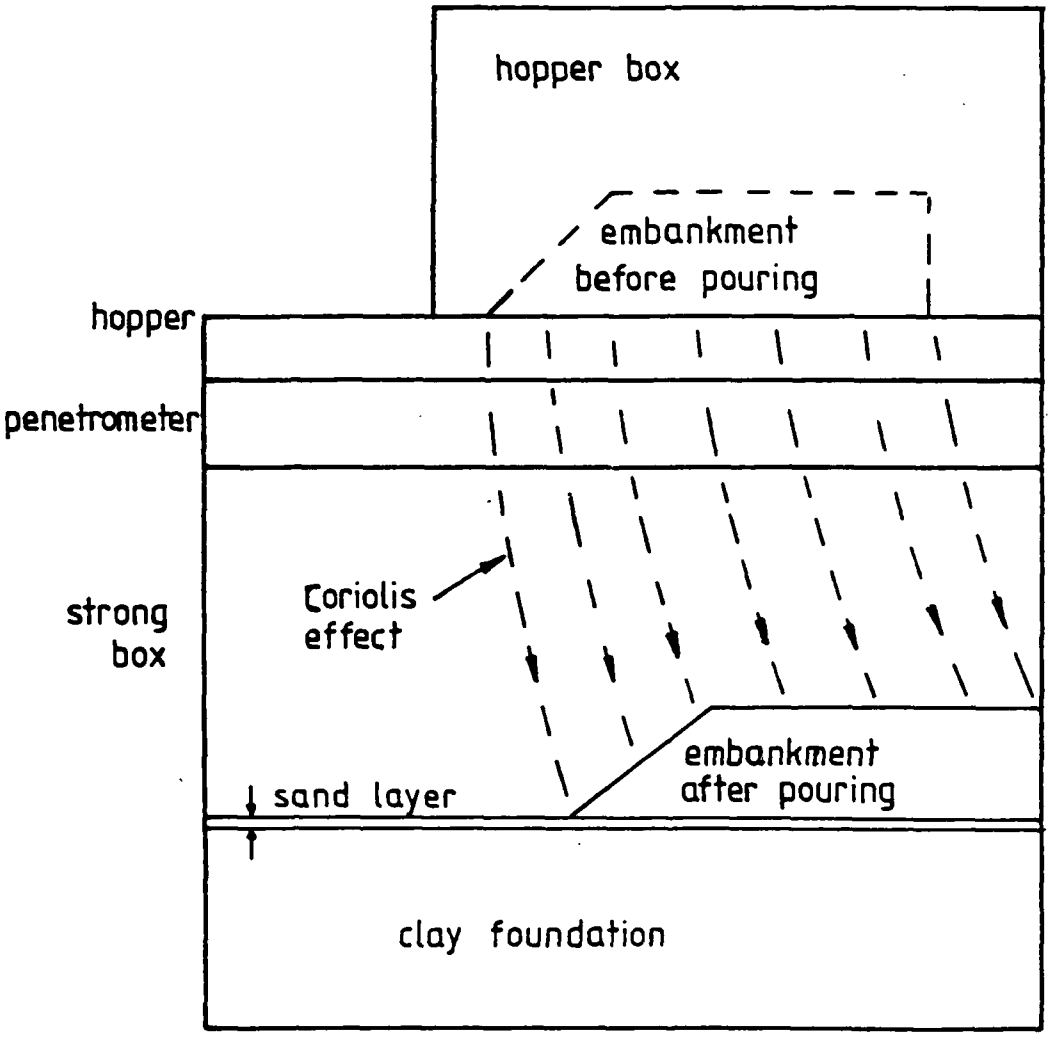

Fig. 2.17 - Embankment construction: Coriolis effect, schematic view

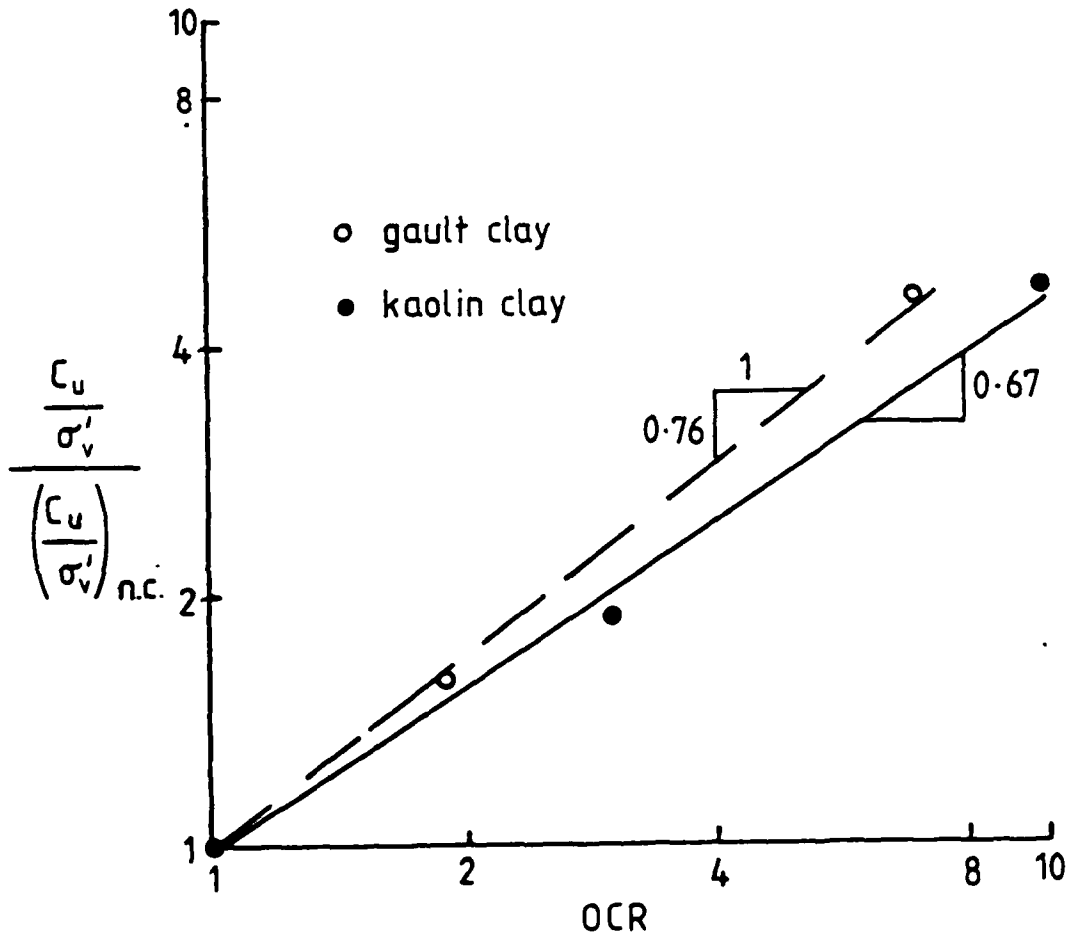

Fig. 3.1 - Vane strength measured in laboratory (after Almeida and Parry, 1983)

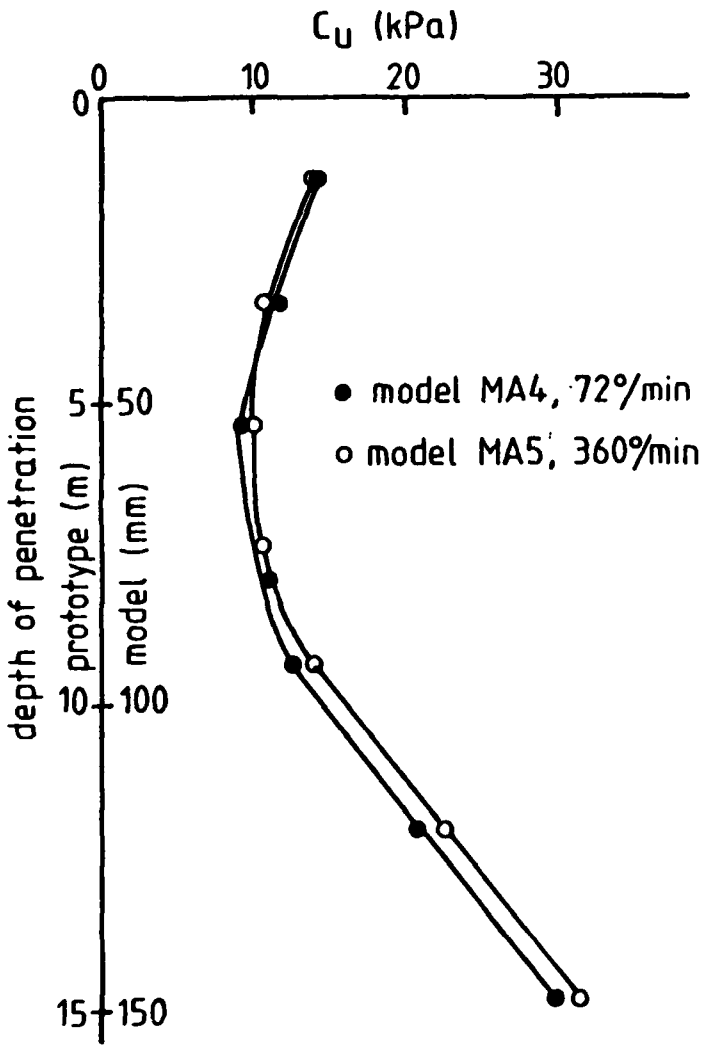

Fig. 3.2 - Influence of the rate of rotation in vane tests

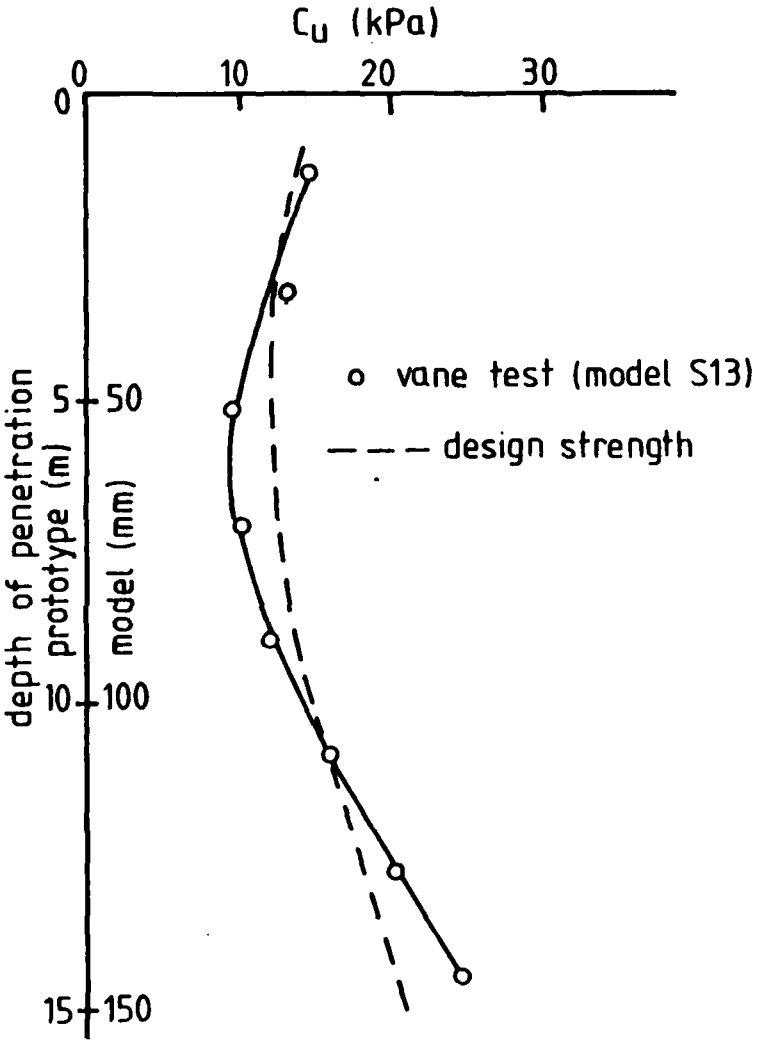

Fig. 3.3 - Predicted and measured undrained strengths

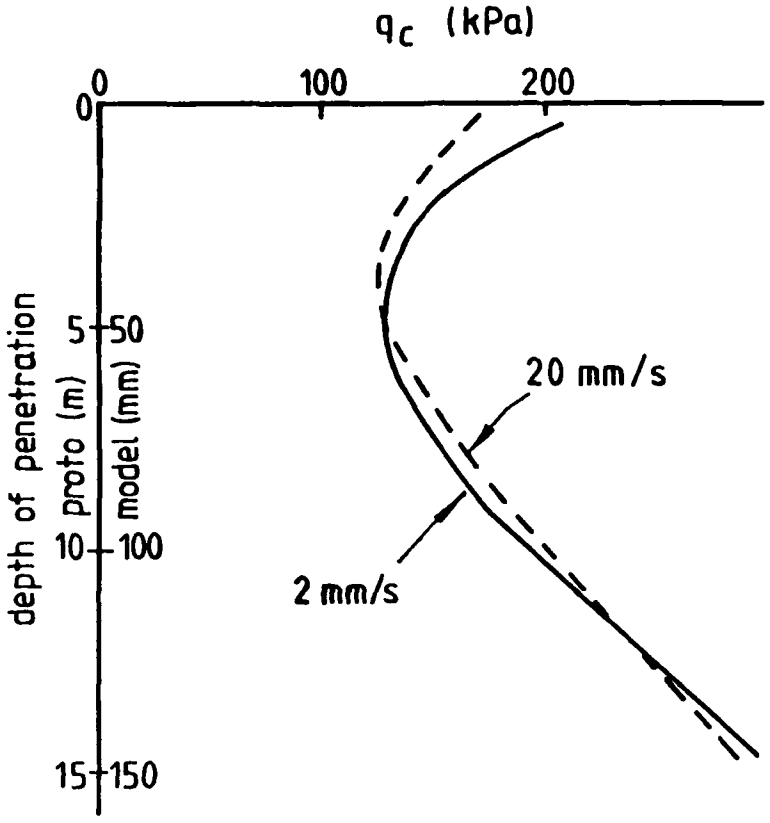

Fig. 3.4 - Influence of the rate of penetration - model SI3

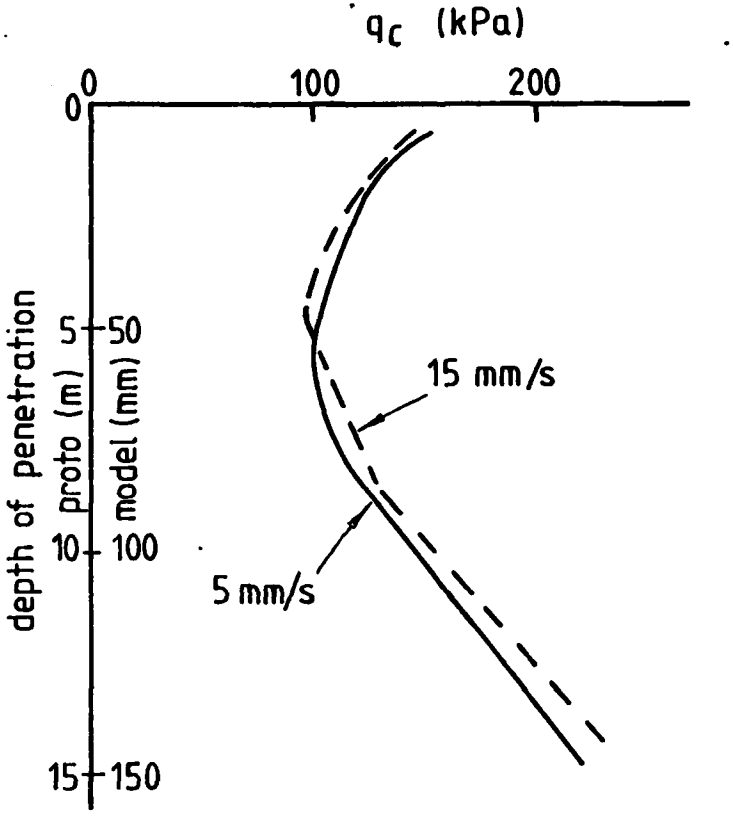

Fig. 3.5 - Influence of the rate of penetration - model MA5

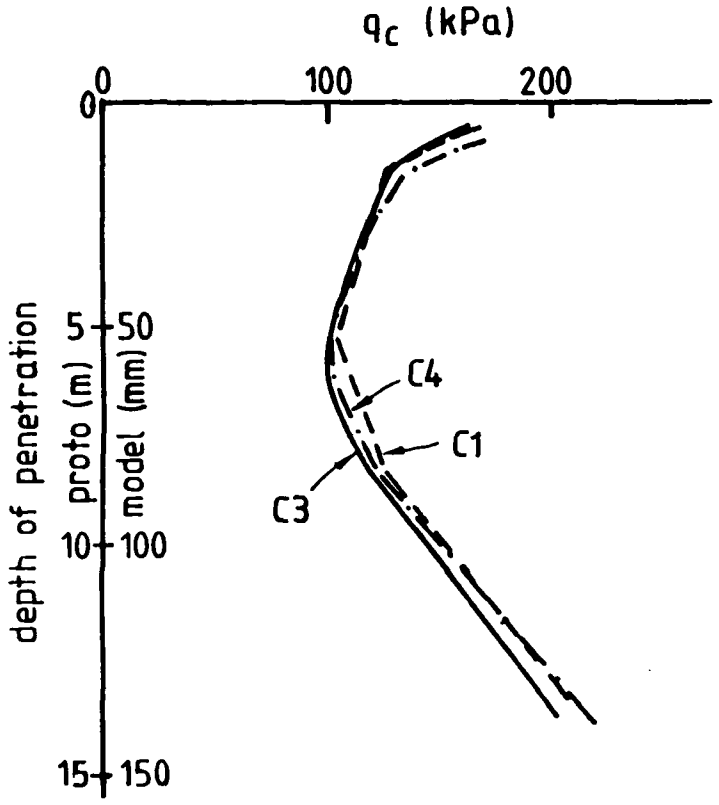

Fig. 3.6 - Penetrometer tests at different locations in plane - model MA5

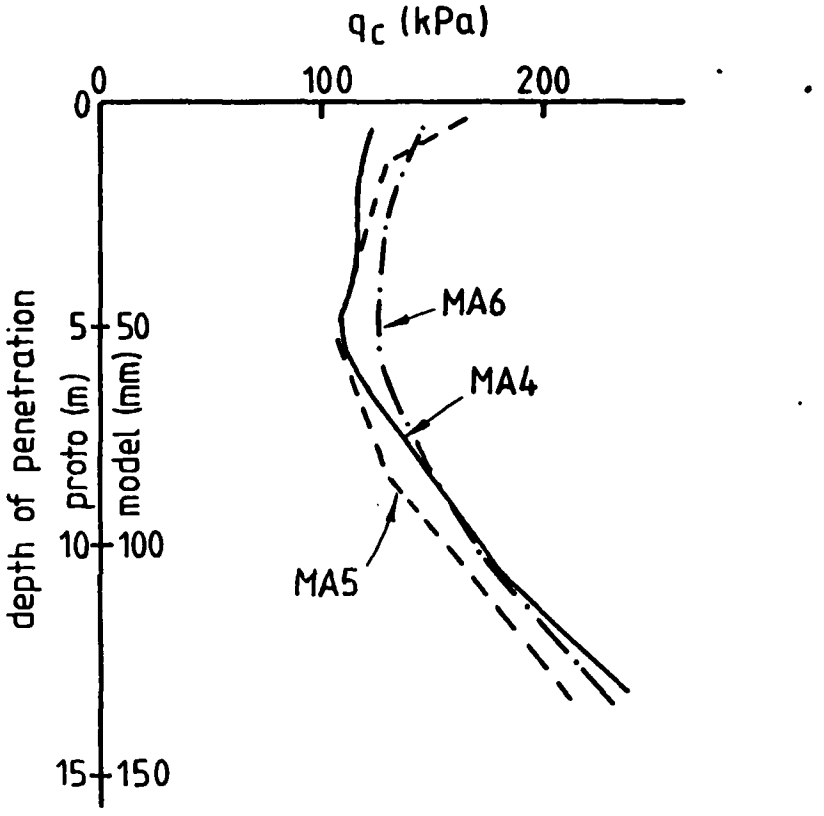

Fig. 3.7 - Penetrometer tests performed in different clay models with penetrometer Mark III

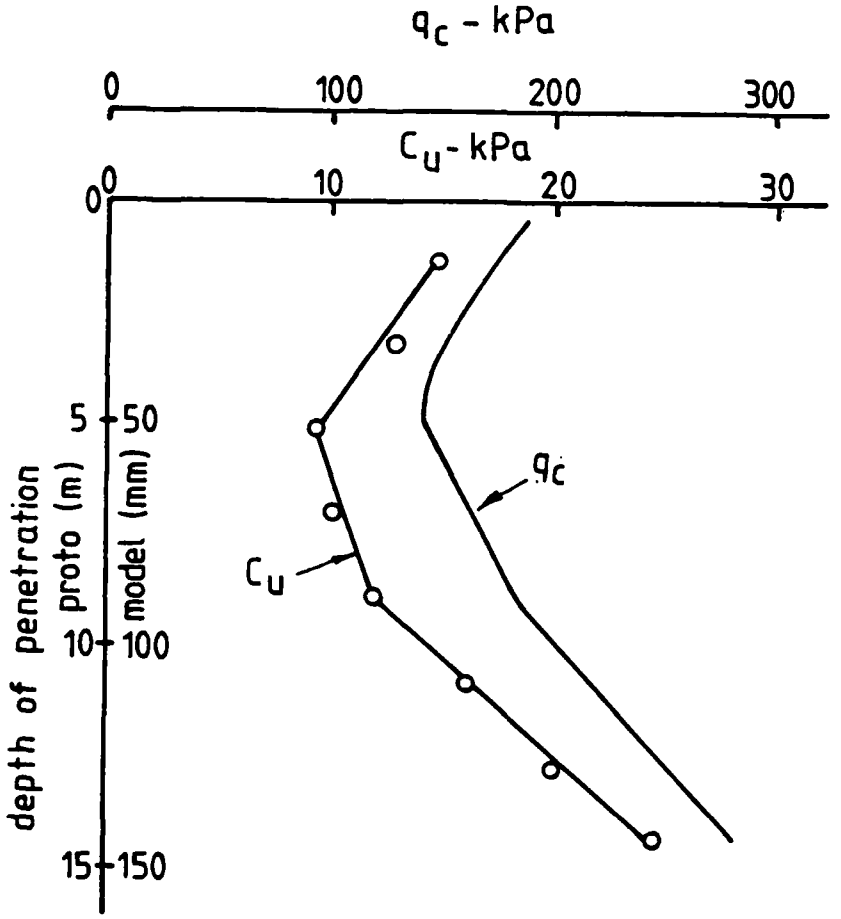

Fig. 3.8 - Penetrometer and vane tests in model SI3

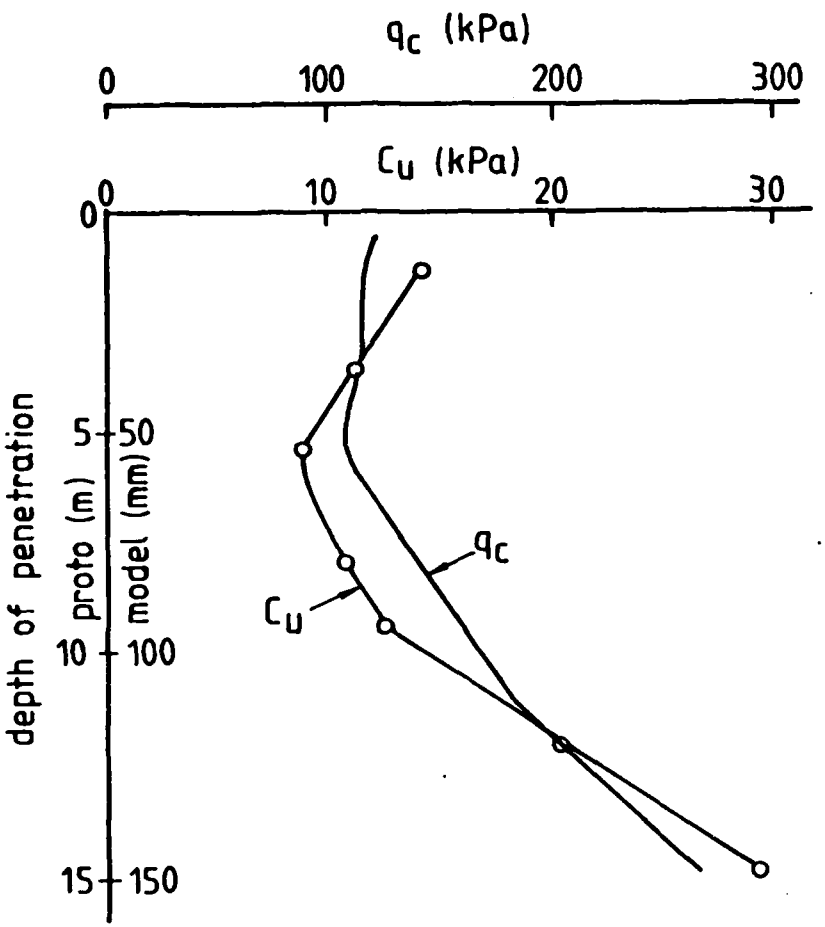

Fig. 3.9 - Penetrometer and vane tests in model MA4

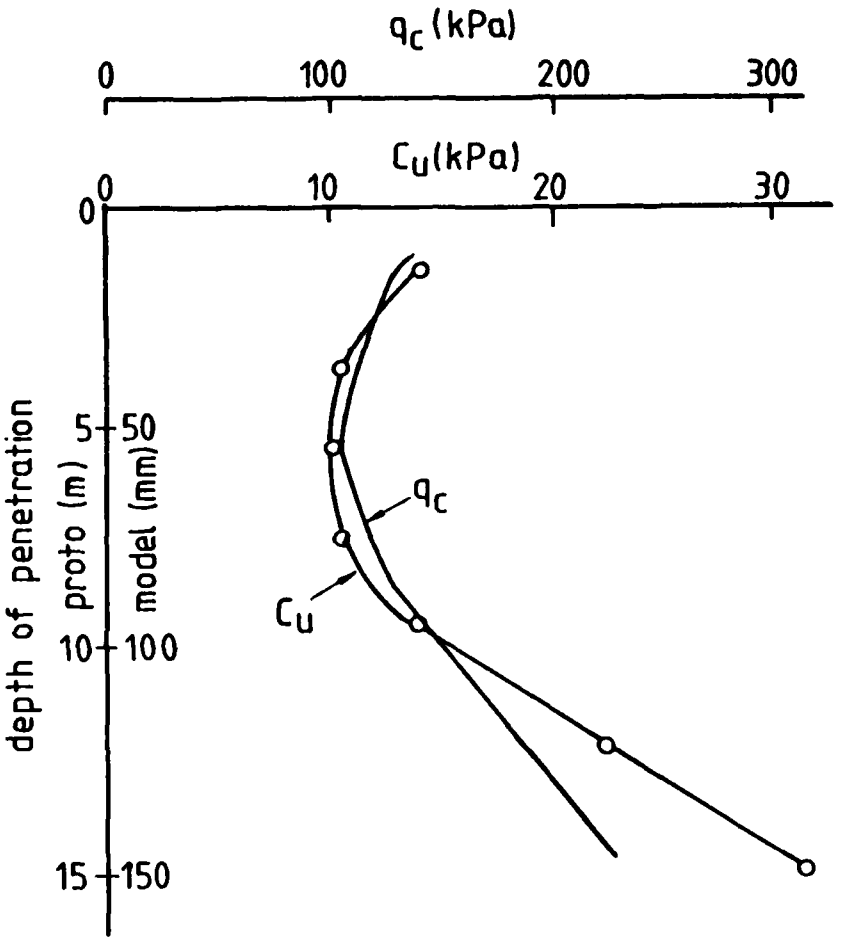

Fig. 3.10 - Penetrometer and vane tests in model MA5

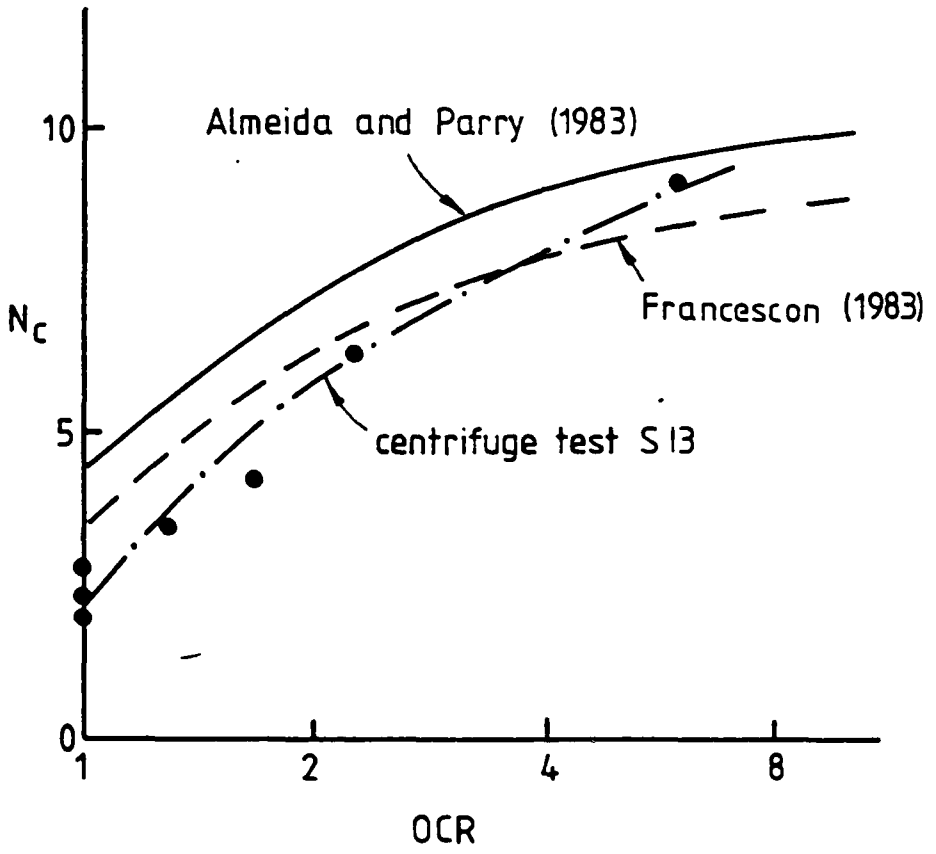

Fig. 3.11 - Values of N_c as measured in laboratory and during centrifuge tests

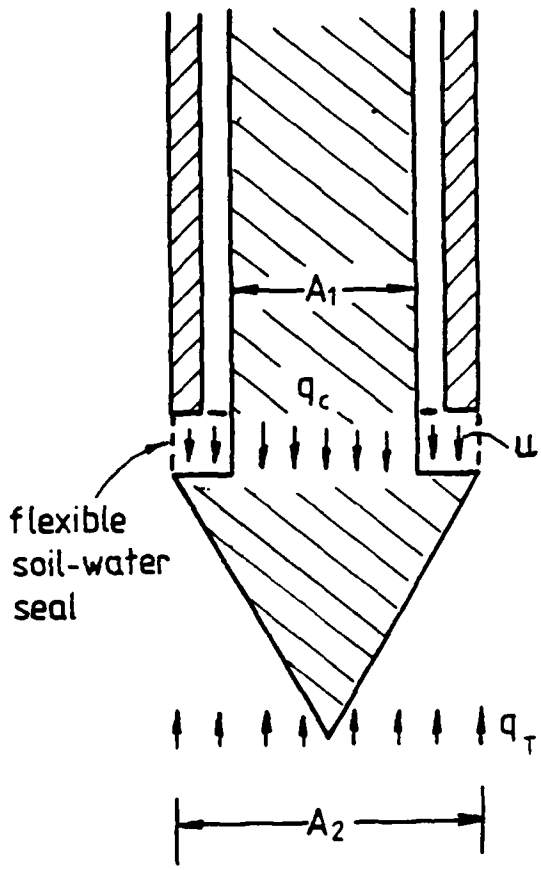

$$a = \frac{A_1}{A_2}$$

Fig. 3.12 - Measured and corrected point resistances

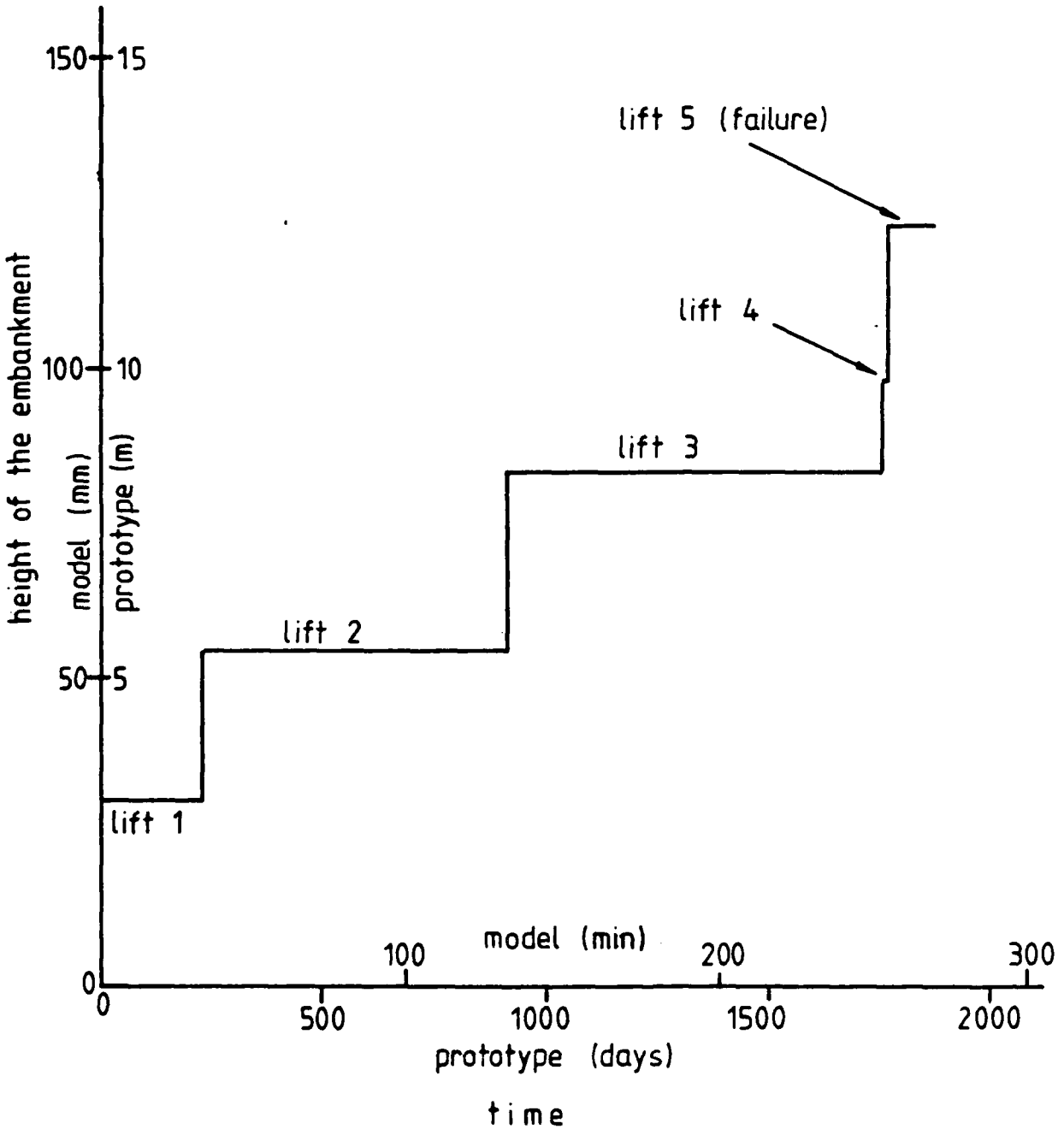

Fig. 4.1 - Loading history during embankment construction: test MA3

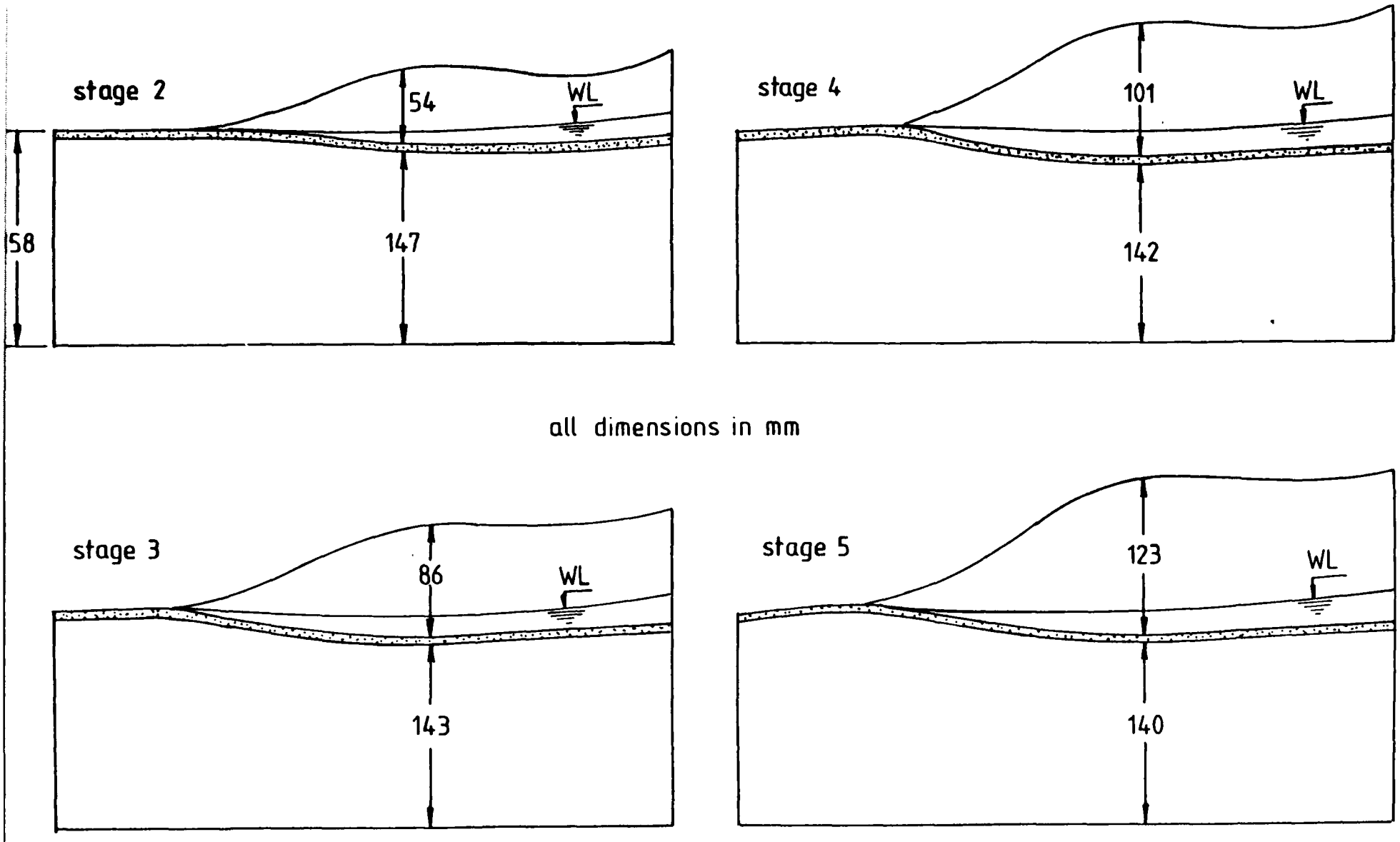

Fig. 4.2 - Embankment geometries during test MA3

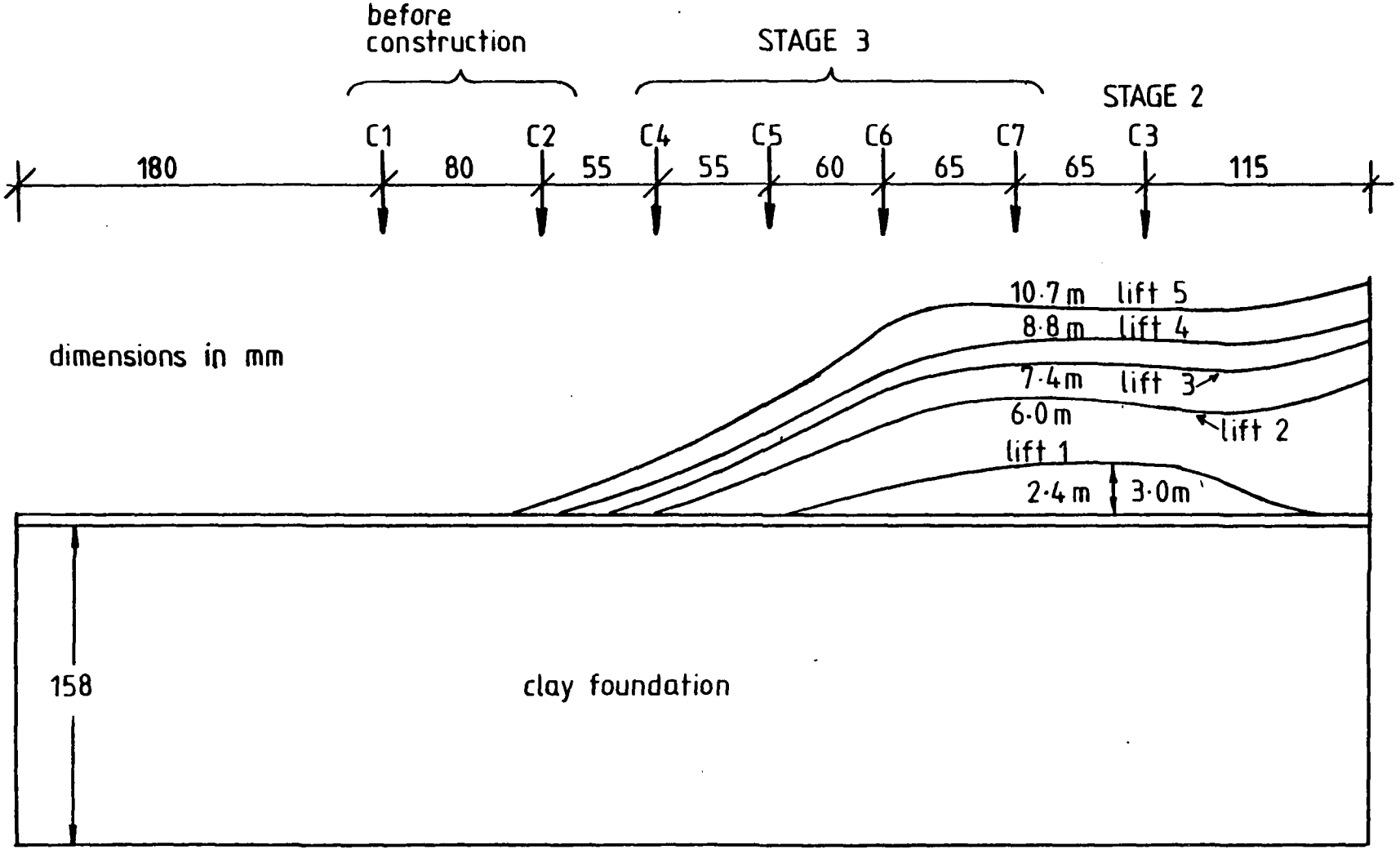

Fig. 4.3 - Location of the penetration tests

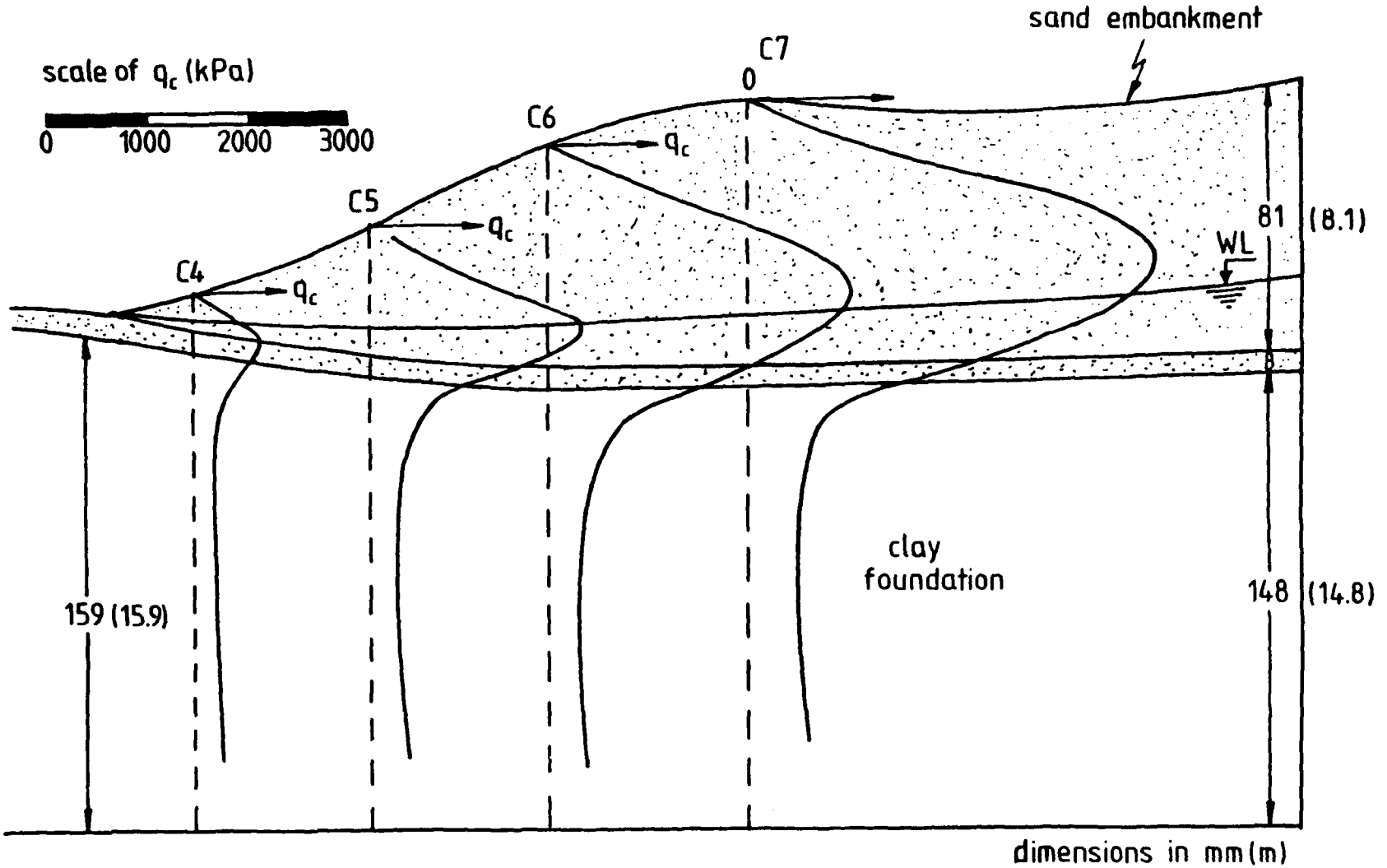

Fig. 4.4 - Cone penetrometer tests C4, C5, C6 and C7 during stage 3, test MA3

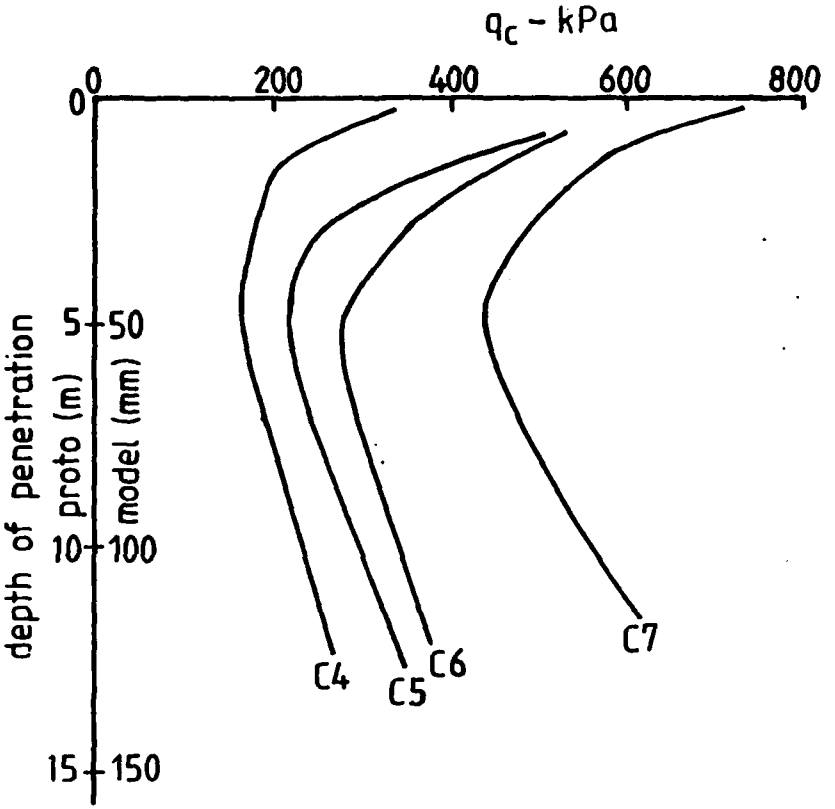

Fig. 4.5 - Cone penetration tests during stage 3

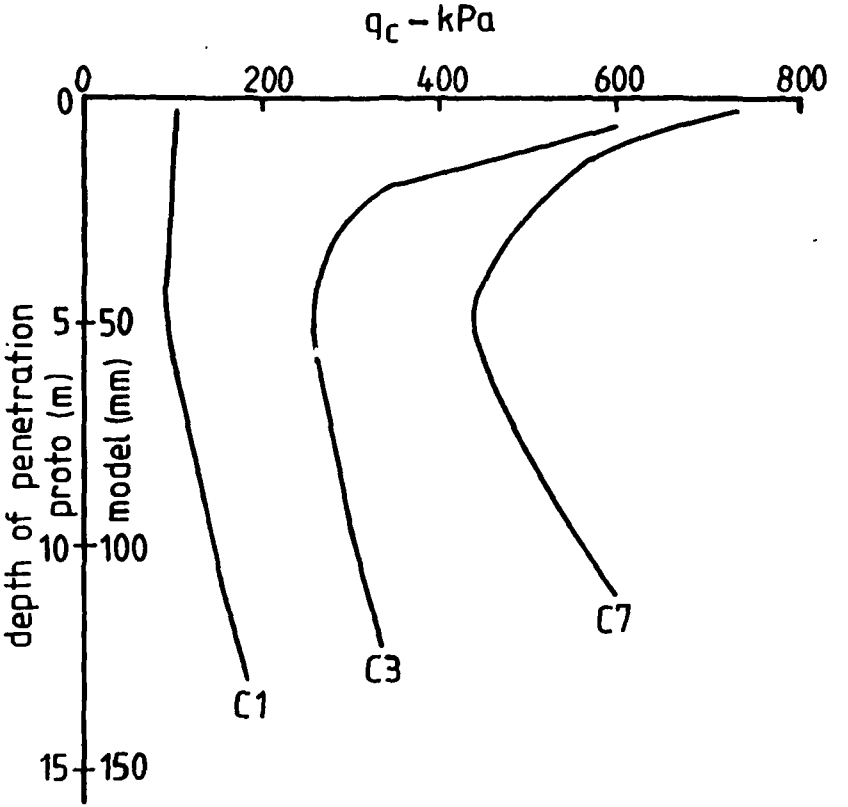

Fig. 4.6 - Cone penetrometer tests in the virgin foundation (C1), during stage 2 (C3) and during stage 3 (C7)

END

FILMED

1-85

DTIC